R. & M. No. 2005
(8073)
A.R.C. Technical Report

MINISTRY OF AIRCRAFT PRODUCTION

AERONAUTICAL RESEARCH COMMITTEE
REPORTS AND MEMORANDA

Tunnel Interference at Compressibility Speeds using the Flexible Walls of the Rectangular High-speed Tunnel

By

C. N. H. Lock, M.A. and J. A. Beavan, M.A.

LONDON: HIS MAJESTY'S STATIONERY OFFICE
Price 6*s.* 6*d.* net

Tunnel Interference at Compressibility Speeds using the Flexible Walls of the Rectangular High-speed Tunnel

By
C. N. H. Lock, M.A. and J. A. Beavan, M.A.,
of the Aerodynamics Division, N.P.L.

Reports and Memoranda No. 2005
27th September, 1944

CONTENTS

1. *Summary.*—The results of various measurements made in the National Physical Laboratory Rectangular High-speed Tunnel using the flexible walls are compared with theory in order to throw further light on the problem of tunnel interference at very high speeds.

The dependence of the wall pressures and overall aerofoil forces on the wall shape has been investigated for two-dimensional tests of various aerofoils, though most of the work relates only to the low drag section EC 1250.

It is concluded that the standard methods of " streamlining " the walls to simulate free air conditions are satisfactory up to speeds at which the shockwave from the aerofoil first reaches one wall, which in ordinary cases occurs above about $M = 0{\cdot}85$ for a low-drag 12 per cent. t/c section, or $0{\cdot}81$ for a conventional 18 per cent. t/c. The 5-in. chord ($c/2h = 0{\cdot}28$) is about as large as should normally be used, and in this case lift can be estimated from the streamline wall pressures, a correction being made for insufficient length of tunnel. If straight walls are used, the theoretical corrections to free air seem applicable up to top speed, and in this case the lift can be obtained from the wall pressures without addition beyond the end of the tunnel.

---

2. *Introduction.*—Since September, 1941, when the aerofoil EC 1250 was first put into the 20 in. × 8 in. Rectangular High-speed Tunnel, a considerable amount of work has been done on it and other aerofoils, especially by wake exploration and surface pressure plotting, subject to the claims of urgent *ad hoc* problems and of the 12-in. Circular Tunnel, which shares the available supply of high pressure air. Besides reports on general progress[1] and shock wave photography[2], notes have been issued giving typical pressure distributions[3] and values of lift and moment[4] of EC 1250, and drag measurements with and without wires to fix transition on NACA 2218 and EC 1250[5]. It is hoped to present a comprehensive report on drag measurements in the near future.

The present note deals with some of the above work and also some special investigations from the point of view of tunnel interference at high speeds, since a good deal of use was made of the flexible walls (*see* Fig. 1 here and Fig. 1 of Ref. 1) during the measurements. Most of the results to be considered are on the EC 1250 section, of which three models of 2-in., 5-in. and 12-in. chord have been available, and on NACA 2218, with which a small amount of work specially connected with tunnel interference has been done.

The theoretical aspect is considered first, beginning with Goldstein and Young's reduction of the compressible to an incompressible case. The theoretical correspondence between the shape of the flexible walls and the pressures along them in the presence of doublets, vortices and sources then leads to the approximate method of setting the walls used as a standard with aerofoils up to the present, together with a proposed modification.

Experimental comparison with theory is made chiefly under two heads : first, the wall pressures when the walls are " straight " (*i.e.* set to have no pressure gradient in the empty tunnel), and the wall shapes required to give constant pressures on the walls when the aerofoil is present ; second, measured differences of C_L, C_M and C_D with different walls.

Finally, the use of the wall pressures to measure C_L is considered.

Theory

3. *Reduction to Incompressible Flow (General).*—A first order theory strictly applicable only as long as none of the flow is supersonic has been developed by Goldstein and Young[7] to relate a compressible flow around an aerofoil to an equivalent incompressible case. The two-dimensional results required in this report are described in that reference under the titles Methods I and II, and may be briefly stated as follows :—

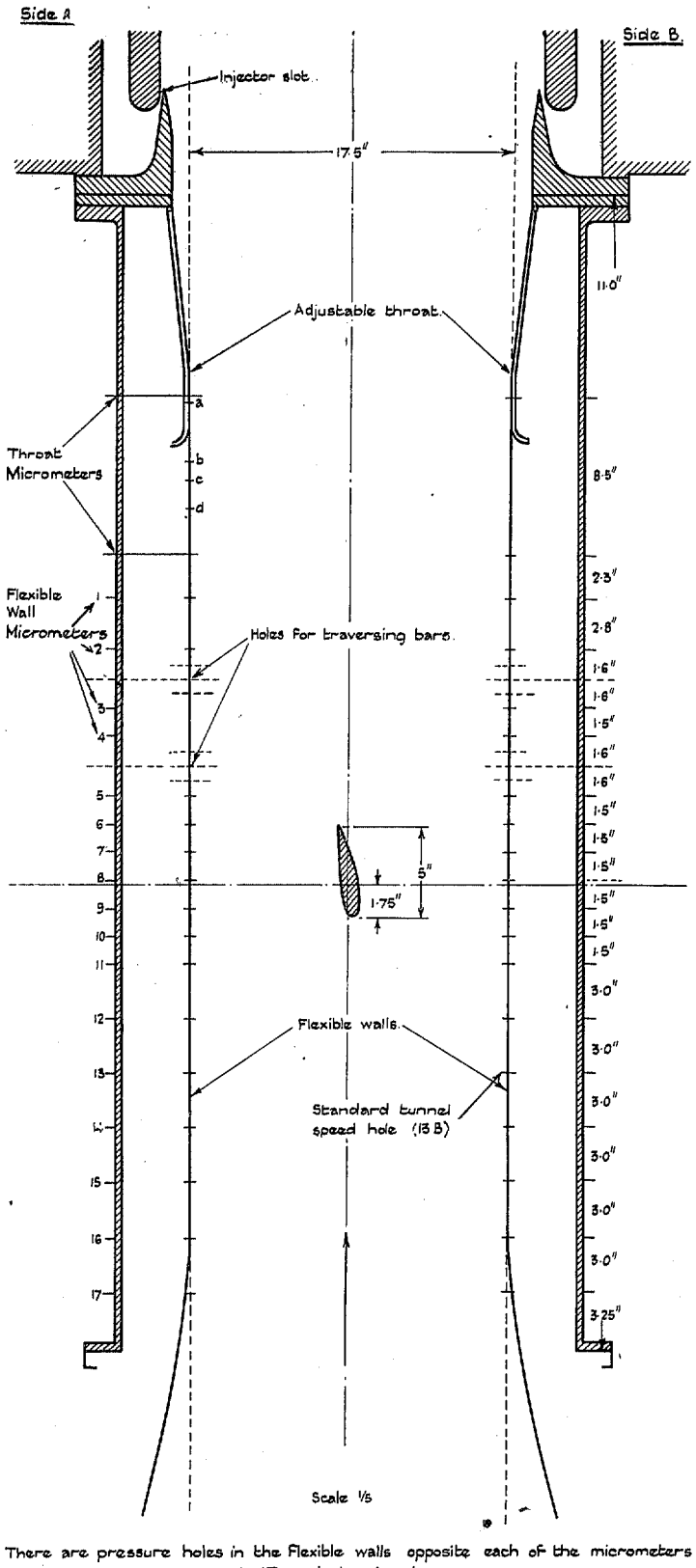

There are pressure holes in the Flexible walls opposite each of the micrometers 1- 17 and at a, b, c, d.

FIG. 1.—Diagrammatic View of the Flexible Walls, Set Straight and Parallel.

Method I.—A compressible flow about a given shape is related to a certain incompressible flow about the *same* shape such that :

(*a*) the streamline at distance h from the axis in the compressible flow is distorted from the straight by the same amount as that at a distance βh and at the same x in the incompressible flow, where $\beta = (1 - M^2)^{1/2}$;

(*b*) the pressure increase at h in the compressible flow is $1/\beta$ times that at βh in the incompressible flow at the same x ;

(*c*) the circulation and lift in the compressible flow is $1/\beta$ times that in the incompressible flow.

Method II.—A compressible flow about a shape β *times as thick* as that in a certain incompressible flow is related to it such that :—

(*a*) the streamline distortion at h in the compressible flow is β times that at βh and at the same x in the incompressible flow ;

(*b*) the pressure increase at (x, h) in the compressible flow is the same as that at $(x, \beta h)$ in the incompressible flow ;

(*c*) the circulation and lift in the compressible flow is the same as that in the incompressible flow.

4. *Streamlines and Pressures for a Doublet, Vortex or Source.*—It is not difficult by a consideration of image systems to prove the following approximate formulae, with $\beta = 1$, for incompressible potential flow for a doublet, a vortex or a source (1) with no walls, (2) with straight walls and (3) with walls adjusted to give constant pressure (Appendix I).

Using the Goldstein and Young formulae[7] " Method II ", the same formulae may be applied to the compressible case by inserting appropriate powers of β in the expression for the coefficient of wall displacement and of change of pressure.

(1) With *no walls*, the introduction of a doublet of strength μ at the origin gives a deflection δ of the streamline $(0, h)$ according to the formula

$$\frac{2\pi Uh}{\mu}\,\delta = -\frac{x^2}{x^2 + \beta^2 h^2} \qquad \ldots\ldots\ldots\ldots\ldots \quad (4\cdot1)$$

and a change of pressure Δp as given by

$$\frac{2\pi U\beta^2 h^2}{\mu}\cdot\frac{\Delta p}{\frac{1}{2}\rho U^2} = \frac{2\beta^2 h^2\,(x^2 - \beta^2 h^2)}{(x^2 + \beta^2 h^2)^2}\,, \qquad \ldots\ldots\ldots \quad (4\cdot2)$$

both to the first order in (μ/Uh^2) considered as a small quantity.

Corresponding values for a vortex of strength K are :—

$$\frac{2\pi U}{\beta K}\,\delta = -\tfrac{1}{2}\log\left\{1 + \left(\frac{x}{\beta h}\right)^2\right\} \qquad \ldots\ldots\ldots\ldots \quad (4\cdot3)$$

and

$$\frac{2\pi U\beta h}{K}\cdot\frac{\Delta p}{\frac{1}{2}\rho U^2} = -\frac{2\beta^2 h^2}{x^2 + \beta^2 h^2}\cdot \qquad \ldots\ldots\ldots\ldots \quad (4\cdot4)$$

For a source of strength m,

$$\frac{2\pi U}{\beta m}\,\delta = \arctan\left(\frac{x}{\beta h}\right) \qquad \ldots\ldots\ldots\ldots\ldots \quad (4\cdot5)$$

and

$$\frac{2\pi U\beta h}{m}\cdot\frac{\Delta p}{\frac{1}{2}\rho U^2} = -\frac{2\beta hx}{x^2 + \beta^2 h^2}\cdot \qquad \ldots\ldots\ldots\ldots \quad (4\cdot6)$$

(2) With *straight walls* $2h$ apart, the pressure variations for the same three examples are :

$$\underline{\text{Doublet :}} \qquad \frac{2\pi U\beta^2h^2}{\mu}\cdot\frac{\Delta p}{\frac{1}{2}\rho U^2} = -\tfrac{1}{2}\pi^2\,\text{sech}^2\,\frac{\pi x}{2\beta h} \qquad .. \quad .. \quad .. \quad (4\cdot7)$$

$$\underline{\text{Vortex :}} \qquad \frac{2\pi U\beta h}{K}\cdot\frac{\Delta p}{\frac{1}{2}\rho U^2} = -\pi\,\text{sech}\,\frac{\pi x}{2\beta h} \qquad .. \quad .. \quad .. \quad .. \quad (4\cdot8)$$

$$\underline{\text{Source :}} \qquad \frac{2\pi U\beta h}{m}\cdot\frac{\Delta p}{\frac{1}{2}\rho U^2} = -\pi\left(\tanh\frac{\pi x}{2\beta h}+1\right) \qquad .. \quad .. \quad .. \quad (4\cdot9)$$

(3) With *constant pressures* along the wall, corresponding to an ideal open-jet tunnel, the deflection of the upper wall assumed to pass through the point $(0, h)$ is given by :

$$\underline{\text{Doublet :}} \qquad \frac{2\pi Uh}{\mu}\cdot\delta = \tfrac{1}{2}\pi\left(\text{sech}\,\frac{\pi x}{2\beta h}-1\right) \qquad .. \quad .. \quad .. \quad .. \quad (4\cdot10)$$

$$\underline{\text{Vortex :}} \qquad \frac{2\pi U}{\beta K}\cdot\delta = -\frac{\pi x}{2\beta h} - \log_e\cosh\frac{\pi x}{2\beta h} \qquad .. \quad .. \quad .. \quad (4\cdot11)$$

$$\underline{\text{Source :}} \qquad \frac{2\pi U}{\beta m}\cdot\delta = gd^*\left(\frac{\pi x}{2\beta h}\right).$$

Values of the above coefficients are given in the following Table 1 and plotted in Fig. 2.

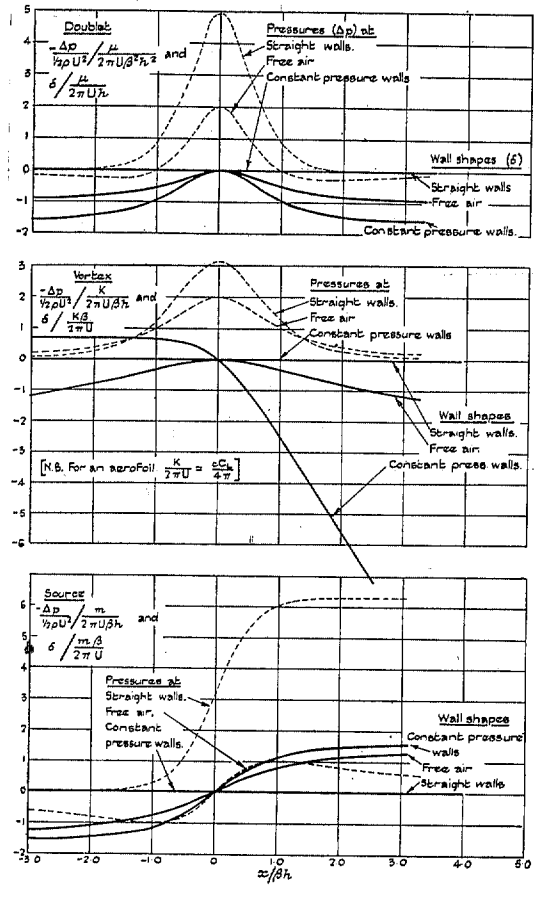

FIG. 2.—Streamlines and Pressures about Doublets, Vortices and Sources.
(*See* also Table 1).

---

* gd stands for the Gudermannian function, alternative definitions of which are $\theta = gdX$, if $\tan\theta = \sinh X$ or $X = \log_e\tan\left(\frac{\pi}{4}+\frac{1}{2}\theta\right)\left(-\frac{\pi}{2}<\theta<\frac{\pi}{2}\right)$.

TABLE 1

Deflection δ

$x/\beta h$	Doublet $\delta \Big/ \frac{\mu}{2\pi U h}$		Vortex $\delta \Big/ \frac{K\beta}{2\pi U}$		Source $\delta \Big/ \frac{m\beta}{2\pi U}$	
	No Walls	Const. Press. Walls	No Walls	Const. Press. Walls	No Walls	Const. Press. Walls
(Upstream)						
$-\infty$	−1·000	−1·571	$-\infty$	0·693	−1·571	−1·571
−3·0	−0·900	−1·544	−1·151	0·693	−1·249	−1·541
−2·5	−0·862	−1·510	−0·991	0·693	−1·190	−1·521
−2·0	−0·800	−1·437	−0·805	0·691	−1·107	−1·476
−1·5	−0·692	−1·277	−0·589	0·684	−0·983	−1·376
−1·0	−0·500	−0·945	−0·347	0·651	−0·785	−1·147
−0·5	−0·200	−0·385	−0·112	0·505	−0·464	−0·713
−0·2	−0·038	−0·074	−0·020	0·265	−0·197	−0·308
0	0	0	0	0	0	0
0·2	−0·038	−0·074	−0·020	−0·363	0·197	0·308
0·5	−0·200	−0·385	−0·112	−1·067	0·464	0·713
1·0	−0·500	−0·945	−0·347	−2·491	0·785	1·147
1·5	−0·692	−1·277	−0·589	−4·029	0·983	1·376
2·0	−0·800	−1·437	−0·805	−5·593	1·107	1·476
2·5	−0·862	−1·510	−0·991	−7·162	1·190	1·521
3·0	−0·900	−1·544	−1·151	−8·733	1·249	1·541
∞	−1·000	−1·571	$-\infty$	$-\infty$	1·571	1·571
(Downstream)						

Pressure Variation Δp

$x/\beta h$	Doublet $-\frac{\Delta p}{\frac{1}{2}\rho U^2} \Big/ \frac{\mu}{2\pi U \beta^2 h^2}$		Vortex $-\frac{\Delta p}{\frac{1}{2}\rho U^2} \Big/ \frac{K}{2\pi U \beta h}$		Source $-\frac{\Delta p}{\frac{1}{2}\rho U^2} \Big/ \frac{m}{2\pi U \beta h}$	
	Straight Walls	No Walls	Straight Walls	No Walls	Straight Walls	No Walls
(Upstream)						
$-\infty$	0	0	0	0	0	0
−3·0	0·006	−0·160	0·057	0·200	0·001	−0·600
−2·5	0·010	−0·200	0·124	0·276	0·002	−0·690
−2·0	0·038	−0·240	0·271	0·400	0·012	−0·800
−1·5	0·176	−0·237	0·590	0·616	0·056	−0·923
−1·0	0·785	0	1·253	1·000	0·260	−1·000
−0·5	2·816	0·960	2·373	1·600	1·082	−0·800
−0·2	4·470	1·776	2·994	1·923	2·186	−0·385
0	4·935	2·000	3·142	2·000	3·142	0
0·2	4·470	1·776	2·994	1·923	4·098	0·385
0·5	2·816	0·960	2·373	1·600	5·202	0·800
1·0	0·785	0	1·253	1·000	6·024	1·000
1·5	0·176	−0·237	0·590	0·616	6·228	0·923
2·0	0·038	−0·240	0·271	0·400	6·272	0·800
2·5	0·010	−0·200	0·124	0·276	6·282	0·690
3·0	0·006	−0·160	0·057	0·200	6·283	0·600
∞	0	0	0	0	6·284	0
(Downstream)						

5. *Tunnel Wall Setting.*—It is clear that the ideal setting of the tunnel walls in the presence of an aerofoil would be obtained if they were of the same shape as the streamlines of the flow in an unlimited stream, an allowance being made for gradually thickening wall boundary layer by increase of the width. If the aerofoil could be replaced by a known system of doublets, vortices and sources it would be possible by the above equations to calculate this ideal setting at each Mach number ; but in general, of course, this system is quite unknown.

5.1. *Original Method for Zero Lift.*—The method that has been in standard use up to a recent date for zero lift is based on some early theoretical work of Taylor and Goldstein (*see* Appendix II) proving that for compressible flow past a corrugated wall analysable into a Fourier series, the pressure variations along a straight wall parallel to it are twice those at the same points in absence of the wall ; so that the free air setting should be made to give half the pressure variations on the straight wall. Assuming linearity between pressures and tunnel width for such small changes as concern us, it was taken that it would be sufficient to set the walls half way between the straight and the position for uniform pressures. As this is much more convenient in practice, it was adopted as a standard method, experimental settings of the walls for uniform pressures being obtained as a preliminary.

5.2. *Original Method for Finite Lift.*—It is evident from Fig. 2 (vortex, constant pressure walls) and on general grounds that level pressures equal on the two walls can only be attained when lift is present by bending the axis of the tunnel through a finite angle θ which depends on the lift coefficient according to the relation

$$\theta = c\, C_L/4h$$

to the first order in C_L. Such a shape cannot be imitated in the existing tunnel and the following alternative scheme was adopted. The pressures were adjusted to constant values along the walls *differing* on the two sides of the tunnel, the value of the difference depending on the lift as explained below in the discussion of experimental results. The walls were then set to a position half way between straight walls and level pressure walls as in the case of zero lift.

5.3. *Revised Method of Wall Setting.*—It appears from Fig. 2 that the above method is not correct for either of the zero lift cases, but that a displacement factor of 0·6 would be more nearly correct for both doublet and source near the aerofoil than the previous factor of 0·5. For finite lift, the *free stream* wall shape for a vortex (Fig. 2) can be imitated without difficulty by the flexible walls over their available length in spite of the logarithmic infinity (equation 4·3). It is proposed, therefore, in future, to adopt the following method which combines an empirical correction for " blockage " with a calculated correction for lift.

With the aerofoil at its test incidence the walls are first experimentally set for constant pressures (unequal on the two sides). Then 0·6 times the *mean* change of the two sides from the " straight " condition of uniform pressures in the empty tunnel is added to the latter, together with an amount, positive on one side, negative on the other, calculated by equation 4·3 for a single vortex in free air based on the estimated lift coefficient at the particular Mach number concerned. The lift will usually be known to a sufficient accuracy from preliminary tests, either by pressure plotting or by integration of the wall pressures (*see* § 11 below).

It must be emphasized that there is as yet no theoretical guarantee that this procedure is the best when there are extensive shock waves present. Comparisons of measured wall pressure distributions with calculated (discussed below in connection with Fig. 10 for example) have shown that even when extensive shock waves are in existence the effect of the aerofoil may actually be represented at almost the highest speeds by equivalent simple doublets, vortices and sources, so that it seems safe to assume that the method is at least a fair approximation to the ideal.

6. *Theoretical Correction of Lift, Drag and Pitching Moment for Straight Walls.*—Formulae are given in R. & M. 1909[7] for corrections to force coefficients measured in compressible flow in a straight-walled tunnel, and the relevant expressions are repeated here for convenience.

If C_L, C_M, D, are values measured in the tunnel at incidence α and Mach number M, then the corrected values for an unlimited stream are $C_L + \Delta C_L$, $C_M + \Delta C_M$, D_0 at Mach number $M + \Delta M$, where

$$\Delta C_L = -\frac{1}{\beta^2}\frac{\pi^2}{24}\left(\frac{c}{2h}\right)^2 (C_L + 2C_M)$$

$$\Delta C_M = \frac{1}{\beta^2}\frac{\pi^2}{192}\left(\frac{c}{2h}\right)^2 C_L$$

$$\frac{D}{D_0} = 1 + \frac{1}{\beta^3}\frac{\pi^2}{6}\lambda\left(\frac{t}{2h}\right)^2 + \frac{1}{\beta^3}2\eta\left(\frac{t}{2h}\right)$$

$$\Delta M = \frac{1}{\beta^3}M\left(1 + \frac{1}{5}M^2\right)\left\{\frac{\pi^2}{12}\lambda\left(\frac{t}{2h}\right)^2 + \eta\frac{t}{2h}\right\},$$

in which h is the half width of the tunnel; c and t the chord and thickness of the aerofoil; λ depends on the shape of the aerofoil (R. & M. 1566[8], pages 53–4); η is an empirical factor (R. & M. 1566[8], pages 56–7); and β as before $= (1 - M^2)^{1/2}$.

Experimental Results

7. *Wall Pressures with Straight Walls.*—During the course of the general work in the tunnel, in which nearly all model tests are normally done with streamline wall settings (*see* § 5), a series of measurements of the pressures at the walls was taken with the EC 1250 model 5-in. chord, at 0 deg., 2 deg. and 4 deg., using settings which give no pressure drop in the absence of the model. These settings, which will be designated " straight walls ", vary in taper with speed owing to thickening of the tunnel wall boundary layer (on all four walls), and it was necessary to use a range, chosen for convenience as $M = 0{\cdot}574$ (below which there was negligible variation), 0·681, 0·732, 0·784, 0·809, 0·835, and occasionally 0·886. Examples of the wall shapes are given in Fig. 13 (empty tunnel).*

Some similar results are also available on EC 1250, 12-in. chord.

Since for Mach numbers above 0·55 the increment in M is very nearly proportional to the corresponding change in static pressure (Table 4 at the end of the report), an approximate scale of ΔM is appended to most of the following graphs. The results are shown in two ways in Figs. 3–6, where a selection of the wall pressure distributions is drawn, together with the sum and difference of the pressure readings on the two sides, which separates out what may be described as " blockage " and " lift " effects.

Experimental points are shown in some of the cases, for illustration. These need some explanation :—

(1) × and + correspond to positive, and o and □ to negative, settings of the aerofoil (symmetrical) and are some check on each other.

---

* The empty tunnel wall shapes at the highest speeds (above $M = 0{\cdot}8$ approx.) have been found to vary considerably from time to time, as shown by the alternative settings dotted in Fig. 13. This effect has subsequently been determined to be due to condensation under the conditions of low temperature of the high speed air, and is roughly correlated with changes in atmospheric humidity, a greater widening of the tunnel being required for constant pressure when the relative humidity is high.

The empty tunnel settings used in most of the work reported herein were the full line curves of Fig. 13, which were determined when the relative humidity was 80–85 per cent. The dotted curves were for R.H. 63 per cent. for $M = 0{\cdot}886$ and 54 per cent. for $M = 0{\cdot}835$, and since the R.H. for most results appears to have been between 65 and 80 per cent. although detailed knowledge is lacking, the difference is not considered great enough to make it worth while attempting to correct the results further. The error that may exist in, for example, the force coefficient curves of Figs. 27, etc., is probably less than 0·01 on M at the highest speed $M = 0{\cdot}85$.

Since at the lowest humidities that have been available (R.H. about 40 per cent.) the empty tunnel wall shapes at the highest speeds have come down nearly into coincidence with the lower speeds, the advantage of using dry air, by return ducts or otherwise, is evident.

(2) The readings are differences from the pressure p_D at a datum hole of much larger diameter, situated a little upstream of micrometer 15 but in the middle of one of the longer (plane) sides of the tunnel.

(3) Upstream of the aerofoil, one of the micrometers 14 (*see* Fig. 1) was afterwards found to have got out of adjustment (after the " straight " tunnel settings had been obtained) and readings of the pressure at the corresponding hole (there is a pressure hole at each micrometer position) are ignored.

(4) Between holes 5 and 4, and 3 and 2, there are holes in the flexible walls to take wake-tube supporting bars which were not present in these experiments. Hence the pressures at these holes tend to equalize up to the pressure behind the flexible wall, which is some kind of a mean of that along the whole wall in view of the incomplete sealing through these walls (they are constructed of a central 4-in. strip with two flanking 2-in. strips, leaving gaps of about 1/50th inch). The mean curves are drawn with this in mind.

(5) The pressures at the two walls have been meaned for the case of zero incidence (Fig. 3).

It would be expected from theory that the peaks of the blockage curves in Figs. 3–6 would be opposite the mid-point of the aerofoil, but that of the lift in Figs. 4–6 opposite the $\frac{1}{4}$-chord point. In all the figures both these conditions are well fulfilled at the lowest Mach number, considering the limits of experimental accuracy. Both peaks tend to move back at high Mach number.

In Figs. 7 and 8 the results are summarised by plotting " peak " blockage and lift values measured at pressure hole 8 (which lies between $\frac{1}{4}$ and $\frac{1}{2}$ chord) except at high M, where values for the next holes were taken if these were found to exceed the values for hole 8. The effect of using empty tunnel wall settings taken at different speeds is also shown in these figures.

Fig. 9 shows the " wake blockage " in terms of the increase of pressure and velocity at the tunnel walls at a point chosen arbitrarily as far downstream of the centre of the aerofoil as the tunnel speed reference point, hole 13, is upstream.

The theoretical curve for blockage is shown on the peak pressure curve, Fig. 7, as that for a 12 per cent. ellipse at zero incidence. In this case the formulae of Appendix I (4) and Method I of § 3 are applicable for free stream conditions ; and the same ratio of factors as for a doublet (Table 1) has then been used to give the straight wall case. It will be seen from the comparison curve at 0 deg. that this curve is a little lower at the higher speeds than that for a simple doublet of strength μ/β, where μ is chosen to give the same peak wall pressure at zero Mach number as the ellipse. The variation in $\Delta p/\frac{1}{2}\rho U^2$ in the case of such a doublet is proportional to $1/\beta^3$.

Fig. 7 shows that the " total blockage " effect as defined by the peak rise in pressure at the walls opposite the aerofoil only begins to diverge appreciably from that predicted on potential theory about an ellipse when the speed rises above $M = 0{\cdot}7$ ($0{\cdot}65$ for 4 deg.) ; and beyond that, until the highest speeds obtainable are reached (even after the shock wave has reached the wall on one side, in the case of 4 deg.) the curve of rise is smooth. A large part at least of the excess rise can be seen to be due to the increasing importance of the " wake blockage " component. This is best demonstrated in Fig. 10, where sample blockage curves at high speeds have been split up into " solid " and " wake " components, the latter being assumed to be of the form produced by a source as in Fig. 2, placed at the T.E. It will be seen that, if this latter component is large (Fig. 9), as it is when the drag rises, it will add to the solid blockage opposite the centre of the aerofoil (which is all that can be predicted from potential flow about an ellipse), and will also account for most of the backward shift of the peak pressure at the highest speeds. It therefore seems that simple doublet and source systems can be used to replace an aerofoil, as regards blockage, to a very high M. But the alternative analyses in Fig. 10 show that the positioning of the equivalent source is very important, as regards choice of the magnitude of the equivalent doublet.

In Fig. 9, illustrating the growth of the wake effect, the point chosen is far enough down the tunnel for the theoretical velocity increase due to a source at the T.E. to have become constant (Fig. 2). The strength of source for the comparison curves in Fig. 9 is calculated by a method due to Dr. Thom[12] which will be described later (§ 10.1). Agreement is seen to be reasonably good at the highest Mach numbers.

In Fig. 8, comparison theoretical curves for the lift effect on the tunnel wall pressures are given, calculation here being based on a simple vortex of strength appropriate to the C_L actually obtained by simultaneous pressure plotting (the " straight wall " values of Fig. 27). For a constant C_L the rise in $\Delta p/\frac{1}{2}\rho U^2$ would be proportional to $1/\beta$.

Agreement of the experimental results is very good up to speeds well beyond the appearance of shock waves, and not unfavourable right up to the speed at which a wave reaches the wall (§ 11). From Figs. 4–5 it seems also that the length of the tunnel is just about sufficient, integration of the wall pressure difference over its full length giving a fair approximation to the lift as measured by pressure plotting (Fig. 31) (*see* § 12 below).

On the 12-in. chord model (Fig. 6), since interference effects at incidence were expected to be too large for useful analysis, the results are mainly at no lift, with one case only at 1 deg.

The data for the peak pressure curve are very scanty in this case but are shown in Fig. 11, again with an ellipse for comparison. The difference of 20 per cent. between observed and calculated curves is perhaps a measure of the extent to which a 12-in. chord aerofoil is too large for the tunnel.

8. *Wall Shapes for Constant Pressures.*—Wall shapes for constant pressures are available for almost all aerofoil tests, since they were necessary as a step in determining the streamline wall shapes.

It has already been noticed (§ 5.2) that when there is a lift on the aerofoil it is impossible to shape the walls of the existing tunnel so as to give constant pressures *equal* on the two walls since this would involve a change of direction of the centre line. In practice it is found that for any given value of the lift there is a particular value of the difference of pressures which is most easy to obtain. Experimental values for all cases recorded are shown in Fig. 12, and for a particular Mach number ($M = 0{\cdot}681$) in Table 2 below. The table gives, in the last column, a value of the length of the tunnel over which the given pressure difference between the two walls would be equal to the lift. It is in all cases of the same order of magnitude as the length of flexible wall available (about 40 in.). This is the probable explanation of the tendency to a particular value of pressure difference which shows a rough correspondence with the lift. Some idea of the variations possible may be gathered from the scatter of the points, and in particular on EC 1250 5-in. chord, for example, at $M = 0{\cdot}835$ and incidence 2 deg. the group of points shows approximately the total range it seemed possible to cover by making special efforts.

TABLE 2 ($M = 0{\cdot}681$)

Aerofoil	$dC_L/d\alpha$ (on Streamline Setting)	Difference of Pressure/α	Length of Tunnel to give Lift
EC 1250			
12-*in. c*	0·08 approx. (Ref. 4)	2·1 in. of water	37 in.
5-*in. c*		1·0	39
2-*in. c*		0·35	44
EC 1250 with 25 *per cent. control* 5-*in. c*			
Control at 0 deg.	0·09 (Ref. 6)	0·8	54
Control at −6 deg.	0·085	0·7—0·85	59—48
Mustang wing section 5-*in. c*	0·13 (Ref. 9) ..	1·45	43
NACA 2218 5-*in. c*	(0·08) (Ref. 10)	0·8	48
Goldstein Roof Top I (*1442/1547*) 5-*in. c* ..	0·12	1·12	52

A difficulty in the way of repeating settings exactly is that a general tilt of the tunnel will clearly make no difference (except a small change, never greater than 0·1 deg., of the incidence of the aerofoil). Further, a small bodily motion of one side parallel to itself should be immaterial, only affecting the difference of pressures between the sides to a very small extent (roughly inversely proportional to the half tunnel width). Both these effects have been experimentally verified in one or two cases.

The pressures were usually made constant from micrometer 16, 20 in. upstream of the aerofoil (*see* scales at the bottom of the figures), to micrometer 1, 15 in. downstream; and as constant as possible beyond, along the leaves of the throat gear[1] a further distance of about 10 in. The procedure, which normally involved simultaneous adjustment of the two sides A and B of the tunnel by separate operators, was to alter the micrometers, working up and down the tunnel, till readings as constant as possible were obtained on all the tubes of the multitube manometer gauge, but to avoid moving micrometer 13B, where the tunnel speed gauge is connected to the corresponding pressure hole.

The observations involved the following models in addition to the EC 1250 5-in. and 12-in. chord included in § 7 (straight walls) :—

Mustang Section[9] of medium thickness $t/c = 14{\cdot}5$ per cent., cambered and designed for low drag. No lift angle $-1{\cdot}3$ deg. at low speed changing to $-1{\cdot}5$ deg. just below the shock stall. Critical Mach number from observed pressures $M = 0{\cdot}69$ at zero lift and 0·65 at 2 deg.

NACA 2218 (section of "Tornado" wing[5]) $t/c = 18$ per cent., low-speed zero lift angle $-1{\cdot}8$ deg. Critical Mach number (calculated) 0·62, 0·635, 0·61 for low-speed C_L 0, 0·1 and 0·2.

To illustrate the actual observations some examples are given (for EC 1250 5-in. chord) without analysis in Fig. 13, a few speeds being taken for each of the cases : no aerofoil, aerofoil at 0 deg., aerofoil at 4 deg. To avoid confusion actual micrometer readings are only shown for one setting in each case. It will be seen that there is some dissymmetry with the empty tunnel, and similarly with the aerofoil present at 0 deg. In the following analysis the corresponding " zero errors " have been subtracted at each speed and each point along the tunnel.

Most of the results have been analysed, much as for the pressures of § 7 (straight walls) into " blockage " and " lift " effects. Thus the blockage curves in Fig. 14 are obtained by taking the mean of the tunnel wall deflections (the displacements from the empty tunnel positions) relative to hole 13 ; and, therefore, give half the increase of tunnel width necessary to keep the velocity along the walls uniform when the aerofoil is present. It should be mentioned that at the higher speeds matters are somewhat critical and consistent results are not always obtainable (*see*, for example, the two curves in Fig. 14 for $M = 0{\cdot}830$ at 4 deg. incidence). The reason may be the uncertainty of the empty tunnel settings at the highest speeds.*

As a more concise method of comparison, the peak values are plotted against tunnel speed in Fig. 20. The corresponding theoretical curve for a 12 per cent. ellipse at 0 deg., calculated for the free air streamlines (Appendix I), is also shown, the assumption being made that the deflections should be corrected to constant pressure walls by the same factor as a doublet (Table 1). The theoretical curve for a single doublet of strength appropriate to the ellipse at low speed gives, as may be seen, somewhat higher values, the difference being due to neglect of second order terms in the aerofoil chord/tunnel width ratio in calculating the equivalence.

Similar curves of blockage (deflections along the tunnel) are given in Figs. 15a and b, and 16, and of blockage (peak values against M) in Figs. 21 and 22, for the " Mustang " and NACA 2218 sections respectively. Figs. 20, 21 and 22 show that the blockage component or general widening of the tunnel past the aerofoil increases smoothly with speed long past the critical of the aerofoil. This is the case with all three aerofoils : the critical low-drag EC 1250, the more practical low-

* *See* footnote on page 8 (§ 7).

drag " Mustang " section, and the conventional NACA 2218. For EC 1250 the curves keep in step with the calculated curves for the ellipse or doublet. The agreement with theory below $M = 0{\cdot}7$ is not so good as with straight walls, but the divergence above this Mach number is similar. The length of tunnel available for setting is now not quite enough (*cf.* the more gradual wall shape curves in Fig. 2 (doublet) with the pressure curves for straight walls).

No explanation is at present offered for (1) the temporary contraction in front of the aerofoil and (2) contraction in the wake region to less than the original width, which both occur at the highest speeds with both the EC 1250 and " Mustang " aerofoils (Figs. 14 and 15). It would seem, however, that these effects must be connected with the general distortion of the pressure distribution everywhere, due to the violent shock waves present at such high speeds.

The separate effect of lift is shown in Figs. 17–22. Since a general tilt of the centre line of the tunnel, which as remarked in the previous paragraph may easily occur in the process of levelling but is too small to affect matters in general, rather obscures a direct comparison of the differences of the micrometers on the two sides, any such occurrence has been eliminated by plotting the mean of the differences at equal distances up and down stream of the $\frac{1}{4}$-chord point. Further, the curves are drawn as deflection of the centre line from a zero at this point. Under these conditions consistent sets of curves are obtained. These would hardly be expected to agree closely with theoretical curves about a single vortex, which require a definite permanent bending of the tunnel to infinity in both directions, but some theoretical cases have been included, mainly to show the agreement with shape of the variation along the tunnel. The absolute magnitude is plotted in Figs. 20–22, where the deflection at an arbitrary distance $9\frac{3}{4}$ in. from the $\frac{1}{4}$-chord point (actually the distance of the tunnel speed hole 13B) has been taken from Figs. 17–19. For EC 1250 this is compared with the theoretical values due to an assumed vortex of strength roughly corresponding to estimated values of the lift at these wall settings (pressure plots giving the precise values of the lift are unfortunately not available).

No theoretical method has been devised of approximating to the case of constant unequal pressures over a finite length of the two tunnel walls ; hence the results for lift are not of much value in elucidating the problem of tunnel interference. The original method of streamline wall setting is best checked (as in § 9 below) by comparison with the newer method.

9. *Wall Shapes and Pressures for Streamline Settings.*—In Figs. 23–26 are shown curves related to the experimental and theoretical pressures and wall shapes for streamline settings on EC 1250 5-in. *c* and 12-in. *c*. Figs. 23 and 24 give wall shapes which are in part the results of some special experiments in which in addition to the standard method of adjusting the wall displacement to a value half way between that for " straight " walls and for constant pressure walls, the walls were set to give pressures half way between the two pressure values (§ 5.1). The figures show good agreement between the two methods on blockage effect even for the 12-in. chord aerofoil ; as regards lift effect, the agreement is not so good but still reasonable.

In both figures the experimental curves are compared with theoretical values in a free stream : those for blockage with an ellipse at 0 deg. and those for lift with the theoretical curves for a vortex of strength appropriate to $C_L = 0{\cdot}33$ for the 5-in. *c* aerofoil at 4 deg. incidence, and to $C_L = 0{\cdot}09$ for the 12-in. *c* aerofoil at 1 deg. The Mach number $M = 0{\cdot}681$ is above the critical value at 4 deg. (approx. $M = 0{\cdot}60$), but below the value for 0 deg. ($M = 0{\cdot}78$) ; the agreement with theory on blockage is good at 0 deg. while at 4 deg. there is an appreciable wake blockage (*see* § 7, Fig. 10, straight walls) which is present to a similar degree for the 12-in. *c* aerofoil at 1 deg. (Fig. 24).

For lift the theoretical and experimental curves diverge both up and downstream of the aerofoil as was to be expected, since the experimental streamline settings are derived by the original method of § 5.2, in which the basic constant pressures are unequal on the two walls.

Fig. 25 reproduces curves of streamline wall pressure distribution for EC 1250 5-in. c at 4 deg. incidence, $M = 0{\cdot}681$ (the condition corresponding to the wall shapes of Fig. 23) ; also experimental curves for straight walls and theoretical curves for straight walls and for free stream. In Fig. 25 the experimental curves compare the original and revised methods of obtaining streamline settings. It is evident that the difference between the two methods is almost within the limits of experimental error. Both experimental and theoretical curves of lift effect illustrate the more gradual dropping off up and downstream for streamline walls as compared with straight walls. There is a further discussion on this point in § 12, in connection with deducing the lift from integration of the wall pressures. The experimental curves agree reasonably well with theory, but the experimental peak suction for straight walls is slightly lower than would be predicted.

As regards blockage, experimental curves have already been compared for straight walls with theoretical curves for a source and doublet (Fig. 10 and discussion in § 7 above).

A much greater range of data is summarised in Fig. 26, in which the observed pressures at hole 8, nearly opposite the centre of EC 1250 are plotted against Mach number for straight walls, streamline walls and constant pressure walls. The observations are separated into " blockage effect " and " lift effect " as in previous cases, and include three values of incidence, 0 deg., 2 deg. and 4 deg.* The observed values for straight walls differ from those given in Figs. 7 and 8 in that the latter are peak pressures which increase continually with M, whereas, since the pressure peak moves backwards at the higher speeds, the curves of Fig. 26, taken at a fixed point on the wall, turn over (*e.g.* at $M = 0{\cdot}82$ for 4 deg. incidence). The results serve to confirm that, for walls adjusted midway between straight and level pressure shape, the pressures lie nearly midway, up to the highest available Mach numbers.

In addition to those illustrated here, a large number of other streamline wall settings are available. For example, the pressures opposite a two-dimensional " Mustang " wing model have been shown to be in similar agreement with theory to those discussed here.

10. *Force Coefficients from Aerofoil Pressure Plottings and Wake Measurements and Their Dependence on Wall Shapes and Relative Size of Model and Tunnel.*—Some early measurements of C_L and C_M by pressure plotting methods showed the dependence of the values obtained on the method of setting the walls.[4] Further evidence of a wider scope is here included to show that Goldstein and Young's formulae (§ 6) appear to apply up to a high Mach number. The sort of variation above this, in the presence of shock waves, may also be seen.

10.1. *Lift.*—In Fig. 27 are plotted curves of lift coefficient against Mach number deduced from the result of pressure plotting on EC 1250 section, 5-in. chord. Curves are given for two values of incidence 2 deg. and 4 deg., each for streamline walls and straight walls. At the bottom of the figure the results for streamline walls are compared with the results for straight walls (1) uncorrected and (2) with the Goldstein correction for ΔC_L and ΔC_M by the formulae quoted in § 6 and (3) with an additional correction for blockage given by Dr. Thom in Reference 12. The latter correction resembles Goldstein's formulae of § 6 as regards ΔM, with values of the coefficients calculated on a semi-theoretical basis. It involves changes in M and C_L given by the formulae

$$\frac{\Delta M}{M} = \left(1 + \tfrac{1}{5} M^2\right) \varepsilon$$

$$\frac{\Delta C_L}{C_L} = -\left(2 - M^2\right) \varepsilon ,$$

where $$\varepsilon = \frac{0{\cdot}045\,\pi \times (\text{cross sectional area of aerofoil})}{\beta^3 h^2} + \frac{c\,C_D}{8\,\beta^2 h}.$$

* For lift effect the results at 2 deg. are plotted on twice the scale of those at 4 deg.

The value of ΔC_L is almost negligible in comparison with ΔM. As explained below in the section on drag coefficient the value of C_D to be taken in the second term in ε is not well defined above the shock stall on account of unknown effects of condensation of moisture, etc. Also the value of C_D to be used should correspond to straight walls and an estimated correction had to be made from the available results for streamline walls. In view of the above limitation, the lift results as corrected for blockage by Thom's formula may be considered to be in reasonable agreement with the values for streamline walls, thus confirming the accuracy of both methods.

10.2. *Pitching Moment.*—Similar results for C_M are shown in Fig. 28. The agreement of the corrected straight wall results with results for streamline wall is reasonably good, as in the case of C_L, although the importance of the correction is less, especially at low speeds.

10.3. *Drag.*—In determining the shape of the profile drag/Mach number curve, from wake traverse observations, it is clearly of great importance to find the dependence, if any, of the character of the very steep rise in drag coefficient which is always obtained round about the shock stall, in the presence of the walls. Theory gives little clue to this problem, but experiments of two kinds are useful.

10.31. *Drag Coefficient : Variation of Tunnel Walls.*—Two tests are described :—

(1) *NACA 2218 5-in. c.*—This fairly thick (18 per cent.) conventional aerofoil has been used for extensive measurements of drag in the H.S.T. for comparison with full-scale tests on a " Tornado "[5]. The traverses were made one chord behind the T.E., the aerofoil being at $-0{\cdot}8$ deg. incidence ($C_L = 0{\cdot}1$ approx. at low speed), at tunnel speeds, as given by the wall pressure at hole 13, 1·7 chords ahead of the L.E., $M = 0{\cdot}574$, $0{\cdot}717$ and $0{\cdot}770$. At each of these speeds runs were made at the three wall settings, " straight," streamline and constant pressures. In order to save time* the settings used were all as for tunnel speed (1·7 chords ahead of the aerofoil) $M = 0{\cdot}732$, but the errors consequent on not having the correct setting when making measurements at other slightly different tunnel speeds does not materially affect the comparison under consideration.

It will be seen (Fig. 29) that the results are consistent and that the streamline curve falls about half-way between the other two. The highest speed reached at the walls was approximately $M = 0{\cdot}85$, on the straight walls (at the tunnel speed of $0{\cdot}77$). In view of the lowness of this value compared with that at which compressibility interference effects may be expected to arise (that is, near $M = 1$) as judged by the evidence of this report, there should be little doubt that the streamline curve of rise should be a good approximation to the true free air curve.

(2) *EC 1250 12-in. c. (Fig. 30).*—Traverses were made $0{\cdot}5$ chord behind the T.E. at zero incidence, but in consequence of the much larger interference effect with this chord as compared with the NACA 2218 aerofoil above, it was not convenient to take the same speeds of test for all three types of wall setting, and suitable values of the speed had to be chosen. As with NACA 2218 the wall settings used were all made at one speed, $M = 0{\cdot}784$ (except for the " low speed " measurements at $M = 0{\cdot}677$, which were taken with the walls set at $M = 0{\cdot}684$). In this case the kind of error in the slope† introduced by using only one setting speed, can be seen from the comparison curve in Fig. 30, determined with streamline walls corresponding nearly enough to each speed of test. The effect is presumably accentuated by the large chord in this case.

---

* In view of the erratic day to day changes now attributed to condensation of moisture discussed in a comprehensive report[11], it was necessary to obtain these results in as quick succession as possible. Complete agreement with other determinations of the drag curve made at considerable time intervals (Ref. 5 for example) was not obtained.

† The position of the beginning of the rise is affected by humidity changes[5], *cf.* previous footnote.

10.32. *Drag Coefficient: Variation of Aerofoil Chord/Tunnel Width Ratio.*—On the same Figs. 29 and 30 are shown the available results of tests with a 2-in. c model of NACA 2218 and 2-in. and 5-in. chord models of EC 1250, the former of these also for the 12-in. Circular Tunnel.

The main conclusion that may, perhaps, be drawn from the comparison is that with streamline walls the drag rise is independent of the Reynolds number, or ratio of aerofoil chord to tunnel width, unless the latter is as great as 0·6 (12-in. chord aerofoil) when there appears to be a possible discrepancy of the order of 0·02 on M. The rate of rise is roughly the same, even in this case.

The drag figures for EC 1250 given here must not be taken as final and too much weight must perhaps not be given to these comparisons. In particular, the high drag measurements on the 5-in. chord to date are few and not very accurate, on account of the humidity difficulties already mentioned and the fact that (possibly due to its very flat pressure gradient and far back transition) the aerofoil is very sensitive to small changes of conditions (for example, cleanliness of the surface). At the time of the measurements, interest was confined mainly to values below the shock stall and the position of that stall, and the considerable labour of obtaining the higher values of the drag was not carried out. They were at that time expected to be more affected by tunnel interference than now seems likely. Further discussion, with forthcoming results, is to be published shortly.

10.33. *Drag Coefficient: Correction for Straight Tunnel Walls.*—Dr. Thom, in a recent note[12], gives formulae for the blockage interference corrections to straight wall tunnel results, including the effect of compressibility. The relevant formulae for drag of the same form as § 10.1 have been applied to the curves of Figs. 29 and 30, and it will be seen that the corrected values lie at Mach numbers somewhat higher than for the streamline, though not so high as for the constant pressure walls.

It may perhaps here be appropriate to mention that the general practice in reducing pitot traverse measurements on 2-in. chord aerofoils in the 12-in. Circular H.S.T., which has rigid walls, has been to take as equivalent speed that at the wall far in advance of the aerofoil increased by 0·4 times the amount by which the speed opposite the aerofoil exceeds this value. (This is an empirical correction deduced from some early tests on two NACA 0020 aerofoils of different chords, 2 in. and 1·2 in.). In view of the nearer position of the tunnel speed holes in the present tests (1·7 chords ahead of the aerofoil L.E. for NACA 2218 and 0·85 chords for EC 1250 12-in. c), it was expected that a similar factor applied to the straight wall results would be too great. In fact, the starred points in Figs. 29 and 30 show that factors of 0·3 and 0·2 respectively are required to give agreement with the streamline curves.

11. *Maximum Speeds at the Walls and Top Speed of Tunnel.*—A Table (3) is appended showing the peak velocities at the wall, for EC 1250 at different incidences, under the conditions of straight wall and streamline setting (new method, § 5.3). It is unfortunate that records of the wall pressures were not taken with all aerofoil tests in the tunnel, but the results in the table extrapolate to determine fairly definitely in most cases a limit of speed corresponding to the aerofoil shock wave extending to the wall, at a " correct " streamline setting, beyond which speed any tests would need very special interpretation. Below this speed it seems from a general consideration of the evidence in this report that the " streamline " methods are a good enough approximation to free air conditions. Results available on other aerofoils are also included.

From the column in Table 3 headed " Maximum speed obtainable," it will be seen that with the particular streamline settings used, the highest tunnel speeds actually obtained were usually below those at which the velocity of sound would be reached at the walls opposite the aerofoil using walls streamlined for those speeds. This is sometimes due to the tunnel choking downstream when running at higher than its setting speed, but may also be caused by the aerofoil shockwave itself. It is unfortunate that insufficient wall pressures were read to determine which was usually the case (there are difficulties in taking these readings under the critical conditions occurring near the speed of sound).

From a consideration of Table 3, it seems safe to say that tests with streamline walls on low drag aerofoils of 5-in. chord are not likely to be invalidated by the shock wave reaching one wall until the tunnel speed exceeds $M = 0{\cdot}85$ or so for C_L up to $0{\cdot}5$. With the thicker and more conventional section NACA 2218, this figure is probably reduced to about $0{\cdot}81$. (Published results, [4, 5, 6, 9] are within these limits).

As would be expected, a larger chord, as with EC 1250 12-in. c, reduces the critical speed appreciably.

12 *Deduction of C_L from Wall Pressures.*—Certain of the results considered in this report, relating to pressures on the walls, were accompanied by simultaneous determinations of the pressure distributions over the aerofoil. Consequently it is possible to compare directly the lift obtained by integration of the latter with that obtained on the assumption that any force on the aerofoil at right angles to the stream must be transmitted by pressure on the walls, if these be sufficiently long.

With straight walls a test is afforded by the experiments considered in Figs. 4 and 5. Integration of the " lift effect " curves gives values which may be seen in Fig. 31 to compare well in regard to general variation with M, with the simultaneous pressure plotting results (*see* Fig. 27). A possible reason for the discrepancy in absolute values, which is of the order 5 per cent. increasing to 10 per cent, at high M, is that the wall pressure measurements are made only down the centre line of the flexible walls, where the majority of the pressure holes are situated, and it is known from earlier observations on several offset holes that the distribution across the tunnel walls may not be quite uniform. It would seem reasonable to use a factor to correct for such an error.

In the above instance of the use of straight walls, Figs. 4 and 5 show that the length of tunnel is just sufficient to allow the difference of pressures ahead and behind the aerofoil to fall to a negligible value, except possibly at the very highest speeds. (In Fig. 2, for pressures at straight walls about a vortex, the contribution to the area beyond $x = \pm 20$ in., *i.e.* $x/\beta h = \pm 3{\cdot}0$ at $M = 0{\cdot}65$, say, is only about $1{\cdot}1$ per cent.). But the difference of pressures at free air streamlines as may be seen in Fig. 2, falls more gradually, and a very much greater length of tunnel is then required. This is confirmed by the experimental points of Fig. 25 for the revised method ; this figure also shows little difference between the original and revised methods.

It is obviously difficult to be sure of the considerable extra lift to be added beyond the working length ; however, in the case of Fig. 25, for example, the lift from the walls between $17\frac{1}{2}$ in. ahead and $22\frac{1}{2}$ in. behind the midpoint of the aerofoil is $C_L = 0{\cdot}272$ (original method of setting) and $0{\cdot}283$ (revised method), comparing with $0{\cdot}264$ for the theoretical free air flow about a vortex with the same peak value (which actually gives on integration to infinity the $C_L = 0{\cdot}33$ that was obtained experimentally by pressure plotting). Thus a correction on the basis of the theoretical curves, which is the method practised in the U.S.A., gives a fair approximation.

It is interesting to note that in this case, done with some care, the difference between the two sides for constant pressure walls (*cf.* § 9), which came out to be $4{\cdot}0$ in. of water, gives for these same limits $17\frac{1}{2}$ in. up and $22\frac{1}{2}$ in. down tunnel, $C_L = 0{\cdot}332$.

The difference between lift derived from wall pressures and from pressure plotting, which is for straight walls experimentally 5–10 per cent., although theoretically it should be only of the order 1 per cent., and for streamline walls experimentally and theoretically about 20 per cent., might in either case be compensated by an empirical factor.

13. *Tunnel Wall Boundary Layer.*—It is not easy to see how the presence of the aerofoil could affect the boundary layer thickness on the walls, which throughout this report has been tacitly assumed to be the same for all conditions at any particular speed. A proper experimental comparison with the aerofoil in and out of place has not been made, but certain results obtained in pitot exploration of the whole field behind the aerofoil indicate little disturbance, beyond the immediate neighbourhood of the ends of the aerofoil at the glass side walls.

For example, with the aerofoil EC 1250 5-in. chord, at the large incidence of $5\frac{3}{4}$ deg. (theoretical critical speed $M = 0{\cdot}45$ approx.) and with the tunnel set for level pressures at $M = 0{\cdot}68$ for the aerofoil at 0 deg., the loss of total head near one of the glass walls at a distance one chord behind and half a chord to the side (lower surface) was nearly constant at high speeds up to $M = 0{\cdot}82$ and nearly the same as that with the aerofoil at 0 deg. (critical speed $M = 0{\cdot}78$) or with no aerofoil (taken, however, at a different period). The loss in these cases was approximately 1 per cent. of the free stream total head at $0{\cdot}7$ in. from the wall or 5 per cent. at $0{\cdot}2$ in., which would have negligible effects on the mean speed. In the empty tunnel the boundary layer at the flexible walls is rather thinner than that at the straight and parallel glass walls.

The complementary effect of the interference of the glass-wall boundary layer on the aerofoil at its ends was also shown in these tests. In the above case, for example, it was found that at $M = 0{\cdot}835$ conditions were constant beyond a distance of about $1{\cdot}8$ in. from the walls, as indicated by explorations normal to the span.

14. *Conclusions.*—The main conclusions to be drawn from the various investigations here considered may perhaps be roughly summarised as follows.

14.1. To a sufficient order of accuracy, both the original and the revised methods of streamlining the walls are satisfactory and simulate free air conditions about an aerofoil in two-dimensional tests. This may be considered fairly well established by the fact that there is reasonable agreement with theoretical results for potential flow around ellipses, doublets, vortices and sources on—

pressure distributions over straight walls,
shapes of constant pressure walls,
pressure distributions and shapes of streamline walls.

An exception is the " lift component " of the shape of constant pressure walls used in the original method of streamlining, in which the pressures on the two sides are unequal and for which no theoretical results are available. Experiment shows, however, little difference between the lift component of the pressure distributions by the original and revised methods of streamline setting.

14.2. Probably the point of most importance in the present work is in assessing the degree to which tunnel results can be trusted at very high speeds. In this connection the inception of a shock wave on the aerofoil has no particular significance. In fact, it is only when a wave has grown to such an extent that it reaches one wall of the tunnel that trouble arises and the conclusions of § 14.1 are invalidated. The conclusion, that up to this speed there is likely to be little error in the Rectangular H.S.T. provided use is made of the flexible walls in the standard manner, is based on the general consistency between results and theory, although the latter is limited in several respects, especially in that the transition to compressible flow assumes only small changes from a general uniform stream velocity.

Except at abnormal incidence the streamline settings should give reliable free-air data roughly up to $M = 0{\cdot}85$ for a low-drag 12 per cent. t/c section, or $0{\cdot}81$ for a conventional 18 per cent., with the standard size of aerofoil.

14.3. The standard chord, 5 in., is probably as large as can be satisfactory for general tests (lift, moment, drag) in this tunnel, which has a width $17{\cdot}5$ in. between the flexible walls and an approximate length 45 in. for adjustment of their shape. For particular investigations, such as wake traverse drag measurements for example, larger chords even up to 12 in. can be used, with the advantage of increasing the maximum Reynolds number from $1{\cdot}8$ to $4{\cdot}0$ million, but care has to be taken in assessing the speed.

14.4. All observations suggest that " lift " and " blockage " effects are independent even at the highest speeds.

14.5. The tunnel wall boundary layer appears to be little, if at all, dependent on the presence of an aerofoil, at least up to $M = 0{\cdot}82$, and should not affect the conclusions of this report, where its independence has been assumed throughout.

14.6. If a straight wall tunnel (*i.e.* straight apart from being corrected for pressure drop at each speed due to thickening boundary layer on all four walls) of these dimensions is used for aerofoil tests, the theoretical and semi-theoretical formulae of References 7 and 12 seem to be satisfactory for correcting the observed values of lift and moment right up to the limits of § 14.2, despite the restrictions (for example, small changes of velocity) applying to the theory. This is true also for drag deduced from wake traverse, and in addition a method of correcting for straight walls originally applied to the circular tunnel can be made to fit the streamline wall results by a reasonable change of an empirical factor.

14.7. Attempts to deduce the lift of an aerofoil from the distribution of pressure over straight walls show an appreciable discrepancy (of the order 5–10 per cent.) although the length of walls corresponds to a theoretical error of only 1 per cent. This may perhaps be due to departure from truly two-dimensional flow.

For streamline walls the theoretical error is increased to the order of 20 per cent. It is possible that an empirical correction might be satisfactory in both cases.

REFERENCES

No.	*Author*	*Title, etc.*
1	J. A. Beavan and G. A. M. Hyde ..	Interim Report on the Rectangular H.S.T., including some Pitot Traverse Measurements of Drag of the Aerofoil EC 1250. R. & M. 2067. February, 1942.
2	W. F. Hilton	Note on Spark Photography in the 20 in. by 8 in. Rectangular H.S.T. at the N.P.L. 5628. February, 1942. (Unpublished.)
3	J. A. Beavan and G. A. M. Hyde ..	Examples of Pressure Distribution at Compressibility Speeds on EC 1250. R. & M. 2056. September, 1942.
4	J. A. Beavan and G. A. M. Hyde ..	Compressibility Increase of Lift and Moment on EC 1250 for Low-speed C_L 0·17. R. & M. 2055. September, 1942.
5	H. H. Pearcey	Drag Measurements on NACA 2218 Section at Compressibility Speeds for Comparison with Flight Tests and Theory. R. & M. 2093. April, 1943.
6	J. A. Beavan, G. A. M. Hyde and R. G. Fowler	Pressure and Wake Measurements up to Mach Number 0·85 on an EC 1250 Section with 25 per cent. Control. R. & M. 2065. February, 1945.
7	S. Goldstein and A. D. Young	The Linear Perturbation Theory of Compressible Flow, with Application to Wind-tunnel Interference. R. & M. 1909. July, 1943.
8	H. Glauert	Wind-tunnel Interference on Wings, Bodies and Airscrews. R. & M. 1566. September, 1933.
9	J. S. Thompson, M. Markowicz, J. A. Beavan and R. G. Fowler	Pressure Distribution and Wake Traverses on Models of Mustang Wing Section in the R.A.E. and N.P.L. High-speed Tunnels. 8135. R.A.E. Report Aero. 1948. August, 1944. (Unpublished.)
10	W. F. Hilton	High-speed Tunnel Balance Tests on an NACA 2218 Aerofoil. R. & M. 1975. November, 1943.
11	H. H. Pearcey	The Effect of Condensation of Atmospheric Water Vapour on Total Head and Other Measurements in the N.P.L. High-speed Tunnels. 7482. February, 1944. (To be published.)
12	A. Thom	Blockage Corrections and Choking in the R.A.E. High-speed Tunnel. 7361. November, 1943. R.A.E. Report Aero. 1891. (To be published.)
13	R. McKinnon Wood	Streamline Walls in High-speed Tunnels. 7332. January, 1944. (Unpublished.)
14	R. McKinnon Wood	The Boundary Layer, Choking and Expansion of the Flow in High-speed Tunnels. 7334. January, 1944. (Unpublished.)

TABLE 3 (*a*) *Streamline Settings*

Aerofoil	Incidence α (deg.)	Wall Setting Speed M_S	Tunnel Speed M	Maximum Speed opp. Aerofoil M_A	Hence Extrapolation to $M_A = 1$ M and $M_S =$	Maximum Tunnel Speed obtainable on Wall-setting M_S	Remarks
EC 1250 5-in. *c*	0	0·732	0·724	0·739	(above 0·9)		
		0·784	0·777	0·802			
		0·835	0·827	0·861		0·874	
		0·886	0·878	0·883		0·931	
	2	0·784	0·778	0·805			
		0·835	0·833	0·879	(above 0·9)	0·862	
		0·886	0·884	0·915		0·910	
	4	0·732	0·726	0·760			
		0·784	0·777	0·828	0·88		
		0·835	0·827	0·902		0·856	
	6	0·732	0·731	0·783			
		0·784	0·783	0·872	0·83	0·825	
		0·835	0·834	(above 1)		0·849	
EC 1250 5-in. *c* with 25 per cent. control	0, 2, 4, 5, 6 $\eta=0°$				0·90	0·84 for $M_S=0·835$	Maximum speeds very erratic. Higher wall settings than for $M_S=0·855$ not attempted.
					0·90		
					0·88		
					0·86		
					0·84		
	0, $\eta=8°$				0·88	0·85 for $M_S=0·855$	
	2, $\eta=6°$				0·88		
	4, $\eta=-8°$				0·85		
	6, $\eta=-6°$				0·86		
"Mustang" 5-in. *c* (Low-speed no-lift angle −1·5°)						$M_S=$ 0·886 / $M_S=$ 0·835	
	−2				0·86	0·857 0·844	Maximum speeds very erratic
	−1					0·868 0·856	
	0				0·87	0·846 0·844	
	1					0·857 0·849	
	2				0·87	0·869 0·852	
	3					0·851	
	4				0·86	0·838	
	5				0·85	0·820	
NACA 2218 5-in. *c* (Low-speed no-lift angle −1·8°)	−0·8				0·83 approx.		
EC 1250 12-in. *c*	0	0·835	0·805	1·00		0·812 for $M_S=0·835$	Maximum speed is obtained when wall speed becomes supersonic 1 chord behind T.E.

TABLE 3 (*contd.*)

(*b*) *Straight Wall Settings*

Aerofoil	Incidence α (deg.)	Wall Setting Speed M_s	Tunnel Speed M	Maximum Speed opp. Aerofoil M_A	Hence Extrapolation to $M_A = 1$ M and M_s =	Maximum Tunnel Speed obtainable on Wall-setting M_s	Remarks
EC 1250 5-in. *c*	0	0·732 0·784 0·835 0·886	0·738 0·790 0·833	0·775 0·852 0·947	0·85	0·827 0·843 0·877	
	2	0·784 0·835	0·780 0·833	0·855 0·975	0·84	0·838	
	4	0·732 0·784 0·835	0·726 0·773	0·812 0·888	0·82	0·833	
NACA 2218 5-in. *c*	−0·8				0·80 approx.		
EC 1250 12-in. *c* ..	0				0·75		

TABLE 4

Variation of Mach Number with Static Pressure

$$M^2 = \frac{2}{\gamma - 1}\left\{\left(\frac{H}{p}\right)^{\frac{\gamma-1}{\gamma}} - 1\right\} \text{ gives } \frac{dM}{dp} = -\frac{1 + \frac{\gamma - 1}{2M^2}}{\gamma p M}; \text{ and } \gamma = 1{\cdot}4.$$

Hence the change ΔM for a decrease $-\Delta p$ in inches of water is given by

M	0·4	0·45	0·5	0·55	0·6	0·65	0·7
$-\Delta M/\Delta p$ ..	0·00506	0·00467	0·00438	0·00416	0·00400	0·00390	0·00382

M	0·75	0·8	0·85	0·9	0·95	1·0	—
$-\Delta M/\Delta p$ ..	0·00379	0·00378	0·00380	0·00384	0·00390	0·00399	—

APPENDIX I

1. *Potential Flow about a Doublet.*—(*a*) For a single doublet in an infinite stream

$$w \equiv \phi + i\psi = Uz + \frac{\mu}{2\pi z}$$

$$\frac{dw}{dz} = u - iv = U - \frac{\mu}{2\pi z^2}.$$

Hence to the first order in μ/Ur^2 the difference in pressure due to the presence of the doublet is given by

$$\frac{\Delta p}{\frac{1}{2}\rho U^2} = -2\,\frac{u-U}{U} = \frac{\mu}{\pi U}\,\frac{x^2-y^2}{(x^2+y^2)^2}.$$

The streamline $y = h + \delta$ through the point $(0, h)$ is given to the first order in μ by putting $\psi = Uh - (\mu/2\pi h)$ in the relation

$$\phi + i\psi = U(x + ih + i\delta) + \frac{\mu(x - ih)}{2\pi(x^2+h^2)}$$

$$\text{as} \quad \delta = \frac{\mu h}{2\pi(x^2+h^2)U} - \frac{\mu}{2\pi hU} = -\frac{\mu x^2}{2\pi hU(x^2+h^2)}.$$

(*b*) For a single doublet midway between straight walls distance $2h$ apart

$$w \equiv \phi + i\psi = Uz + \frac{\mu}{4h}\coth\frac{\pi z}{2h}.$$

$$\frac{dw}{dz} = u - iv = U - \frac{\pi\mu}{8h^2}\operatorname{cosech}^2\frac{\pi z}{2h}.$$

This represents an infinite series of doublets of the same sign, at the points $x = 0$, $y = 0$, $\pm 2h$, $\pm 4h$, *etc.*

On the wall $z = x + ih$,

$$v = 0,\ u = U + \frac{\pi\mu}{8h^2}\operatorname{sech}^2\frac{\pi x}{2h}$$

$$\frac{\Delta p}{\frac{1}{2}\rho U^2} = -\frac{\pi\mu}{4Uh^2}\operatorname{sech}^2\frac{\pi x}{2h}$$

to the first order if μ/Uh^2 is considered as a small quantity.

(*c*) For a single doublet midway between walls at which pressure and velocity are constant

$$w \equiv \phi + i\psi = Uz + \frac{\mu}{4h}\operatorname{cosech}\frac{\pi z}{2h}.$$

$$\frac{dw}{dz} = u - iv = U - \frac{\pi\mu}{8h^2}\cosh\frac{\pi z}{2h}\Big/\sinh^2\frac{\pi z}{2h}.$$

This represents an infinite series of doublets of alternate sign at the points $x = 0$, $y = 0$, $\pm 2h$, $\pm 4h$, *etc.*

On the wall $z = x + i(h + \delta)$ where δ is the displacement from a straight wall, and $u = U$. Taking μ/Uh^2 to be a small quantity, then to the first order at the wall,

$$w = U(x + ih + i\delta) - \frac{i\mu}{4h}\operatorname{sech}\frac{\pi x}{2h}.$$

Hence the shape of the streamline through the point $(0, h)$, *i.e.*, the shape of the wall is given by

$$\delta = +\frac{\mu}{4hU}\left(\operatorname{sech}\frac{\pi x}{2h} - 1\right).$$

2. *Potential Flow about a Vortex.*—(*a*) For a single vortex in an infinite stream

$$w \equiv \phi + i\psi = Uz + \frac{iK}{2\pi}\log z$$

$$\frac{dw}{dz} = u - iv = U + \frac{iK}{2\pi z}.$$

Hence to the first order in K the difference in pressure due to the vortex is

$$\frac{\Delta p}{\frac{1}{2}\rho U^2} = -2\left(\frac{u-U}{U}\right) = -\frac{K}{\pi U}\cdot\frac{y}{x^2+y^2}.$$

The deflection δ of the streamline through $(0, h)$ is given to the first order in (K/Ur) by putting $\psi = Uh + (K/2\pi)\log h$ in

$$\phi + i\psi = U(x + ih + i\delta) + \frac{iK}{2\pi}\log(x + ih)$$

$$\text{as} \quad \delta = -\frac{K}{4\pi U}\cdot\log\left\{1 + \left(\frac{x}{h}\right)^2\right\}$$

(*b*) Vortex between straight walls, images being of alternate sign,

$$w \equiv \phi + i\psi = Uz + \frac{iK}{2\pi}\log\tanh\frac{\pi z}{4h}$$

$$\frac{dw}{dz} = u - iv = U + \frac{iK}{4h}\operatorname{cosech}\frac{\pi z}{2h}.$$

On the wall

$$v = 0, \; u = U + \frac{K}{4h}\operatorname{sech}\frac{\pi x}{2h}$$

$$\frac{\Delta p}{\frac{1}{2}\rho U^2} = -\frac{K}{2hU}\operatorname{sech}\frac{\pi x}{2h}$$

to the first order in K/hU.

(*c*) Vortex with constant pressure walls, images being of similar sign,

$$w \equiv \phi + i\psi = Uz + \frac{iK}{2\pi}\log\sinh\frac{\pi z}{2h}$$

$$\frac{dw}{dz} = u - iv = U + \frac{iK}{4h}\coth\frac{\pi z}{2h}.$$

On the wall

$$z = x + i(h + \delta), \quad u = U$$

when δ is the deflection of the streamlines, and

$$w = U(x + ih + i\delta) + \frac{iK}{2\pi}\log\cosh\frac{\pi x}{2h} - \tfrac{1}{4}K.$$

Hence the shape of the streamline corresponding to the wall is given by

$$\delta = -\frac{K}{2\pi U}\log\cosh\frac{\pi x}{2h}$$

to the first order.

3. *Potential Flow about a Source.*—In an infinite stream

$$w \equiv \phi + i\psi = Uz + \frac{m}{2\pi}\log z$$

$$\frac{dw}{dz} = u - iv = U + \frac{m}{2\pi z}.$$

To the first order in m the difference of pressure due to the source is

$$\frac{\Delta p}{\frac{1}{2}\rho U^2} = -2\left(\frac{u-U}{U}\right) = -\frac{m}{\pi U}\cdot\frac{x}{x^2+y^2}.$$

The deflection δ of the streamline through $(0, h)$ is given to the first order in m/Ur by putting $\psi = Uh + \frac{1}{4}m$

$$\text{in} \quad \phi + i\psi = U(x + ih + i\delta) + \frac{m}{2\pi}\log(x + ih)$$

$$\text{as} \quad \delta = \frac{m}{2\pi U}\left(\frac{\pi}{2} - \arctan\frac{h}{x}\right) = \frac{m}{2\pi U}\arctan\left(\frac{x}{h}\right).$$

(*b*) Source between straight walls, images all of the same sign,

$$w \equiv \phi + i\psi = Uz + \frac{m}{2\pi}\log\sinh\frac{\pi z}{2h} + \frac{m}{4h}z$$

$$\frac{dw}{dz} = u - iv = U + \frac{m}{4h}\coth\frac{\pi z}{2h} + \frac{m}{4h}.$$

On the wall

$$v = 0,\ u = U + \frac{m}{4h}\tanh\frac{\pi x}{2h} + \frac{m}{4h}$$

$$\frac{\Delta p}{\frac{1}{2}\rho U^2} = -\frac{m}{2hU}\left(\tanh\frac{\pi x}{2h} + 1\right).$$

(*c*) Source with constant pressure walls, images being of alternate sign,

$$w \equiv \phi + i\psi = Uz + \frac{m}{2\pi}\log\tanh\frac{\pi z}{4h}$$

$$\frac{dw}{dz} = u - iv = U + \frac{m}{4h}\operatorname{cosech}\frac{\pi z}{2h}.$$

On the wall

$$z = x + i(h + \delta),\ u = U,$$

where δ is the deflection of the streamline.

$$w = U(x + ih + i\delta) + \frac{m}{2\pi}\log\frac{\sinh(\pi x/4h) + i\cosh(\pi x/4h)}{\cosh(\pi x/4h) + i\sinh(\pi x/4h)}$$

$$= U(x + ih + i\delta) + \frac{im}{2\pi}\theta, \text{ where } \tan\theta = \operatorname{cosech}\frac{\pi x}{2h}$$

$$= U(x + ih + i\delta) + \frac{im}{2\pi}\left(\frac{\pi}{2} - gd\,\frac{\pi x}{2h}\right)^*.$$

Hence

$$\delta = \frac{m}{2\pi U}gd\frac{\pi x}{2h}.$$

---

* *gd* stands for the Gudermannian, one definition of which is $\theta = gd\,X$, if $\tan\theta = \sinh X$.

4. *Potential Flow about an Ellipse at Zero Incidence in an Infinite Stream.*—If a and b are the major and minor semi-axes

$$\psi = Uy - Ub\sqrt{\frac{a+b}{a-b}}\,e^{-\xi}\sin\eta,$$

where
$$\begin{cases} x = \sqrt{a^2-b^2}\cosh\xi\cos\eta \\ y = \sqrt{a^2-b^2}\sinh\xi\sin\eta \end{cases}$$

gives
$$\begin{cases} \dfrac{u}{U} = \dfrac{a}{a-b} - \dfrac{b}{a-b}\left(\dfrac{\sinh\xi\cosh\xi}{\sinh^2\xi+\sin^2\eta}\right) \\ \dfrac{v}{U} = -\dfrac{b}{a-b}\left(\dfrac{\sin\eta\cos\eta}{\sinh^2\xi+\sin^2\eta}\right) \\ \delta = \dfrac{bh}{a+b}\left\{\sqrt{1+\left(\dfrac{a+b}{h}\right)^2\sin^2\eta}-1\right\}. \end{cases}$$

On the y-axis, therefore,

$$\frac{u-U}{U} = \frac{b}{a-b}\left(1-\frac{y}{\sqrt{y^2+a^2-b^2}}\right)$$

and
$$\frac{\Delta p}{\frac{1}{2}\rho U^2} = 1-\left(\frac{u}{U}\right)^2$$

$$\delta = \frac{bh}{a+b}\left\{\sqrt{1+\left(\frac{a+b}{h}\right)^2}-1\right\}.$$

APPENDIX II

Pressures in Compressible Flow past a Corrugated Wall, with and without a Plane Wall. (From some notes of Dr. Goldstein.)

The equations of a compressible flow appropriate to a small (linear) perturbation of a uniform stream, are, with $\beta^2 = 1 + M^2$ as usual,

$$\beta^2\frac{\partial^2\phi}{\partial x^2}+\frac{\partial^2\phi}{\partial y^2}=0,\ u=\frac{\partial\phi}{\partial x};\ v=\frac{\partial\phi}{\partial y}.$$

For flow past a corrugated wall $y = \lambda\cos kx$ in an otherwise unrestricted stream, the solution is

$$\phi = Ux + \frac{\lambda U}{\beta}e^{-\beta ky}\sin kx\ ,$$

giving
$$\frac{p-p_0}{\frac{1}{2}\rho_0 U^2} = -\frac{2(u-U)}{U} = -\frac{2\lambda k}{\beta}e^{-\beta ky}\cos kx \quad .. \quad .. \quad .. \quad (1)$$

to the first order.

For flow between the corrugated wall $y = \lambda\cos kx$ and a plane wall $y = h$,

$$\phi = Ux + \frac{\lambda U}{\beta\sinh\beta kh}\cosh\beta k(y-h)\sin kx$$

giving
$$\frac{p-p_0}{\frac{1}{2}\rho_0 U^2} = -\frac{2\lambda k}{\beta\sinh\beta kh}\cosh\beta k\,(y-h)\cos kx\ . \quad .. \quad .. \quad (2)$$

The ratio of (1) to (2) when $y = h$ is

$$e^{-\beta kh}\sinh\beta kh = \tfrac{1}{2}\,(1-e^{-2\beta kh}).$$

With ordinary values of k and h, this is very nearly $\frac{1}{2}$.

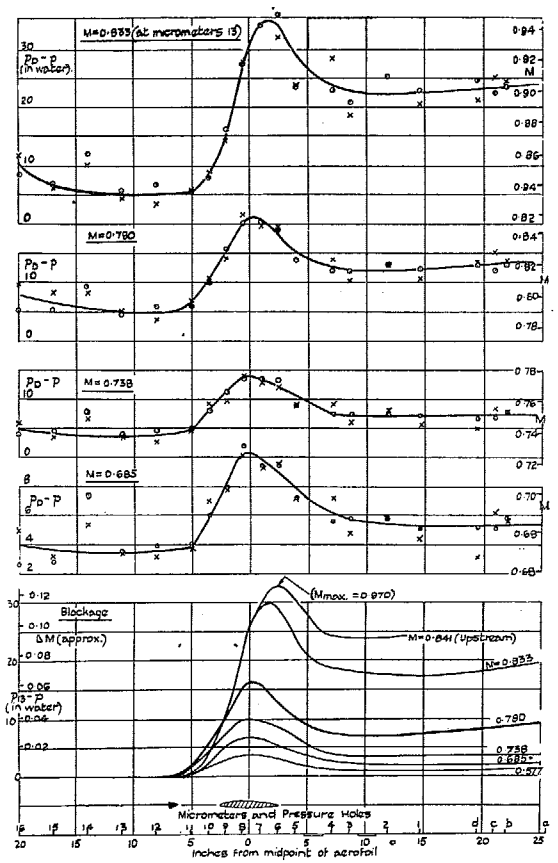

FIG. 3.—Wall Pressures and Velocities with Straight Walls. Aerofoil EC 1250 5-in. chord at 0 deg.

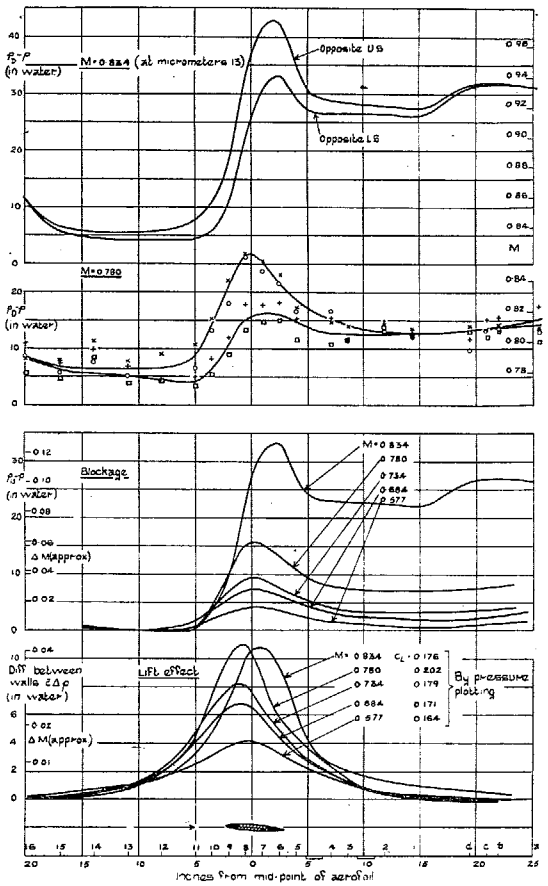

FIG. 4.—Wall Pressures and Velocities with Straight Walls. Aerofoil EC 1250 5-in. chord at 2 deg.

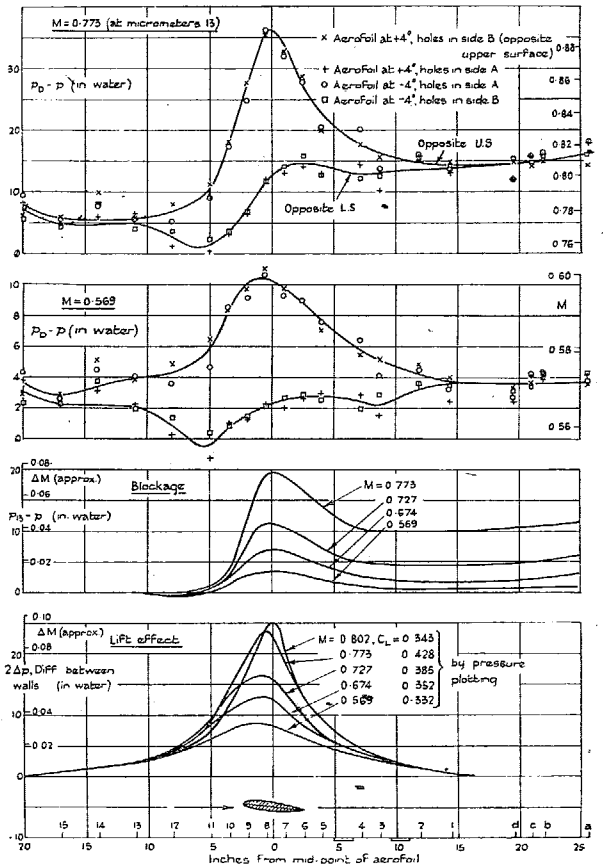

FIG. 5.—Wall Pressures and Velocities with Straight Walls. Aerofoil EC 1250 5-in. chord at 4 deg.

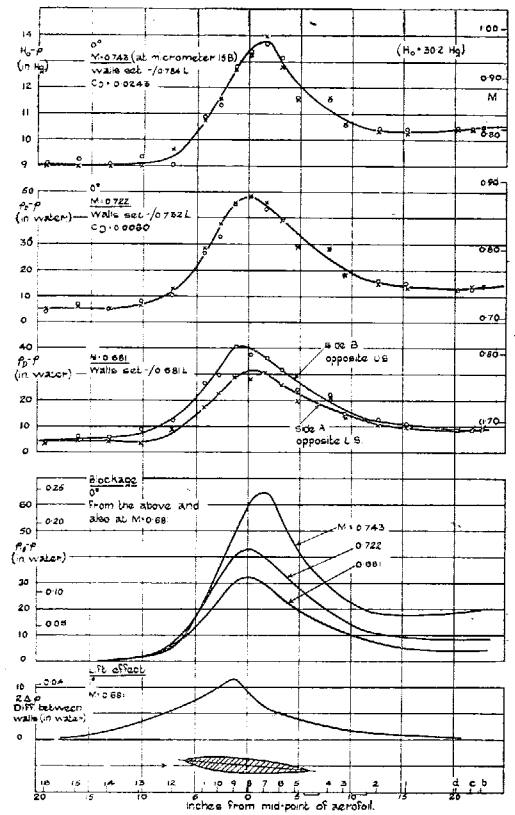

FIG. 6.—Wall Pressures and Velocities with Straight Walls. Aerofoil EC 1250 12-in. chord at 0 deg. and 1 deg.

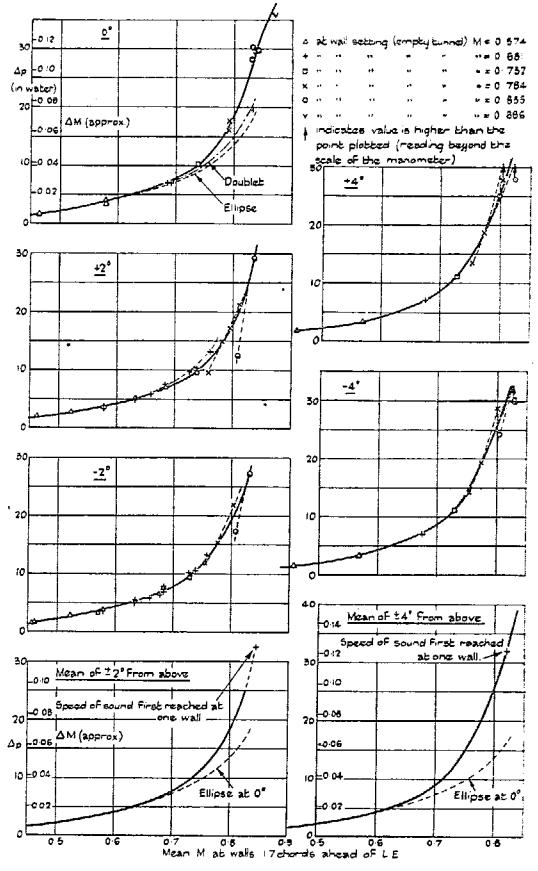

FIG. 7.—Change of Pressure and Velocity opposite Aerofoil EC 1250 5-in. chord on Straight Walls (Blockage Effect).

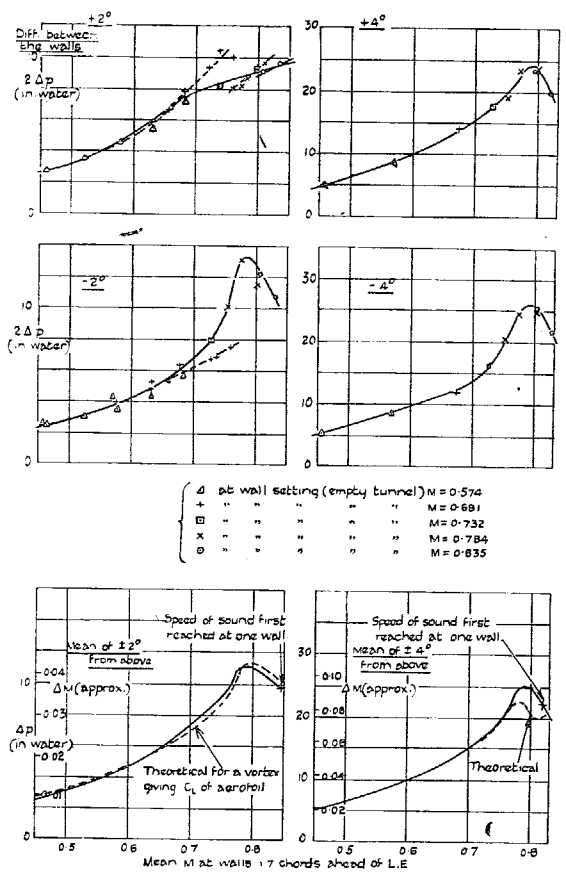

FIG. 8.—Difference of Pressure and Velocity opposite Aerofoil EC 1250 5-in. chord on Straight Walls (Lift Effect).

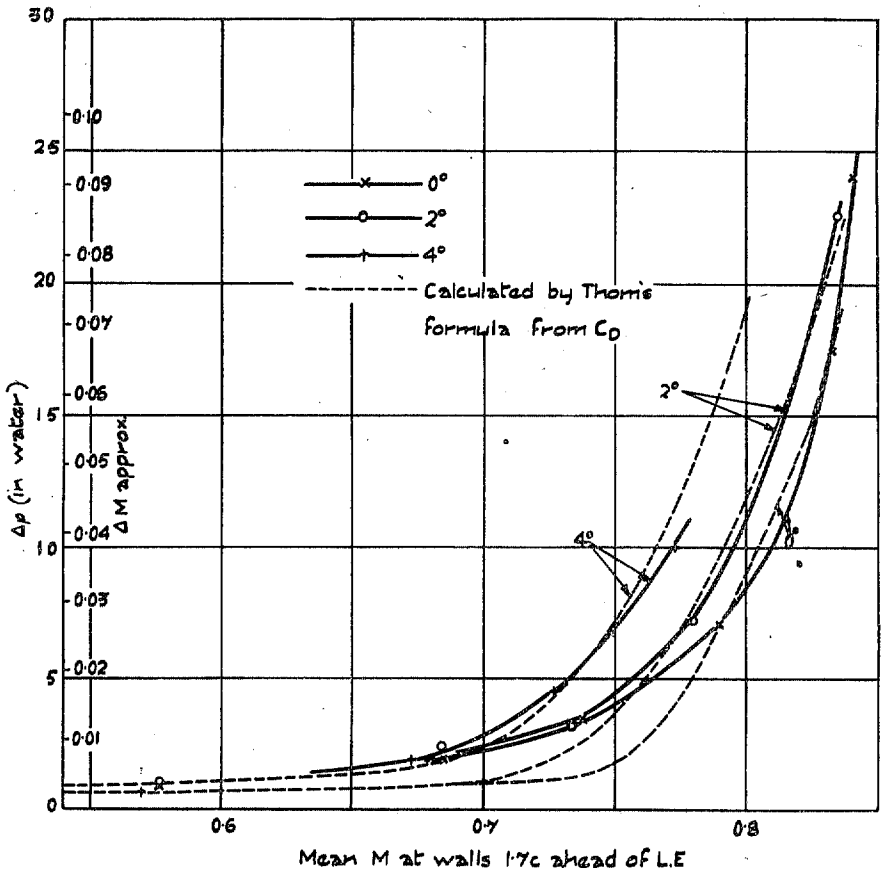

FIG. 9.—Change of Pressure and Velocity behind Aerofoil EC 1250 5-in. chord on Straight Walls. (Wake Blockage Effect; Increase of Velocity at Walls 1·7 *c* behind Trailing Edge.)

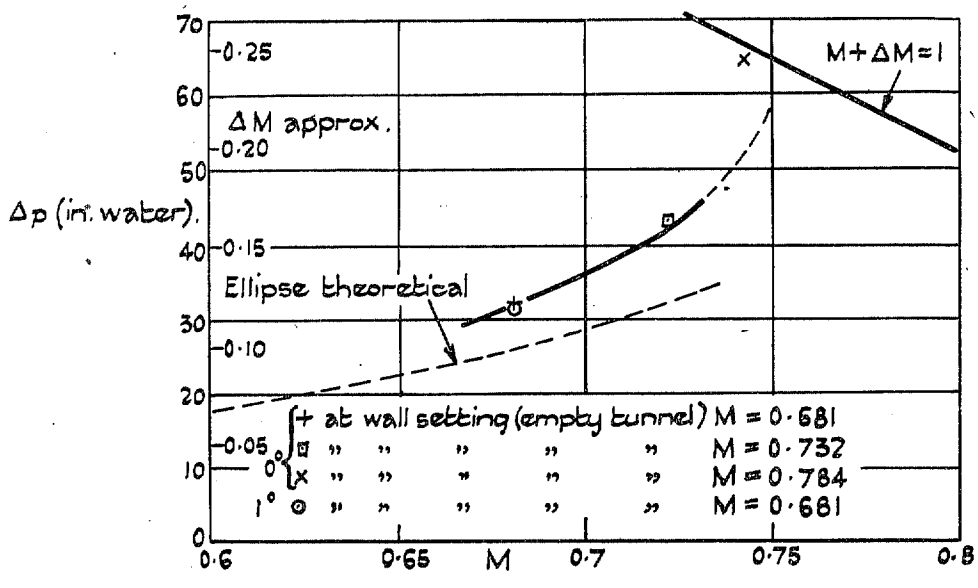

FIG. 11.—Change of Pressure and Velocity opposite Aerofoil EC 1250 12-in. chord on Straight Walls (Blockage Effect).

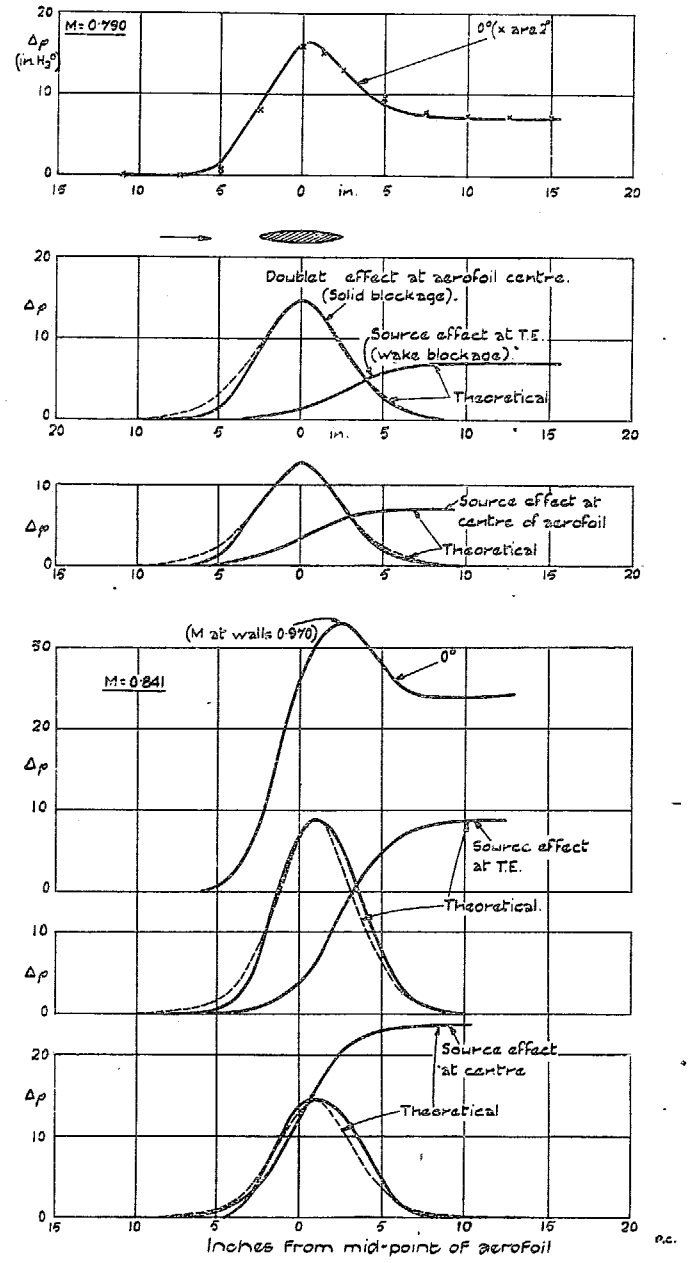

FIG. 10.—Analysis of Blockage into Doublet and Source Effects.

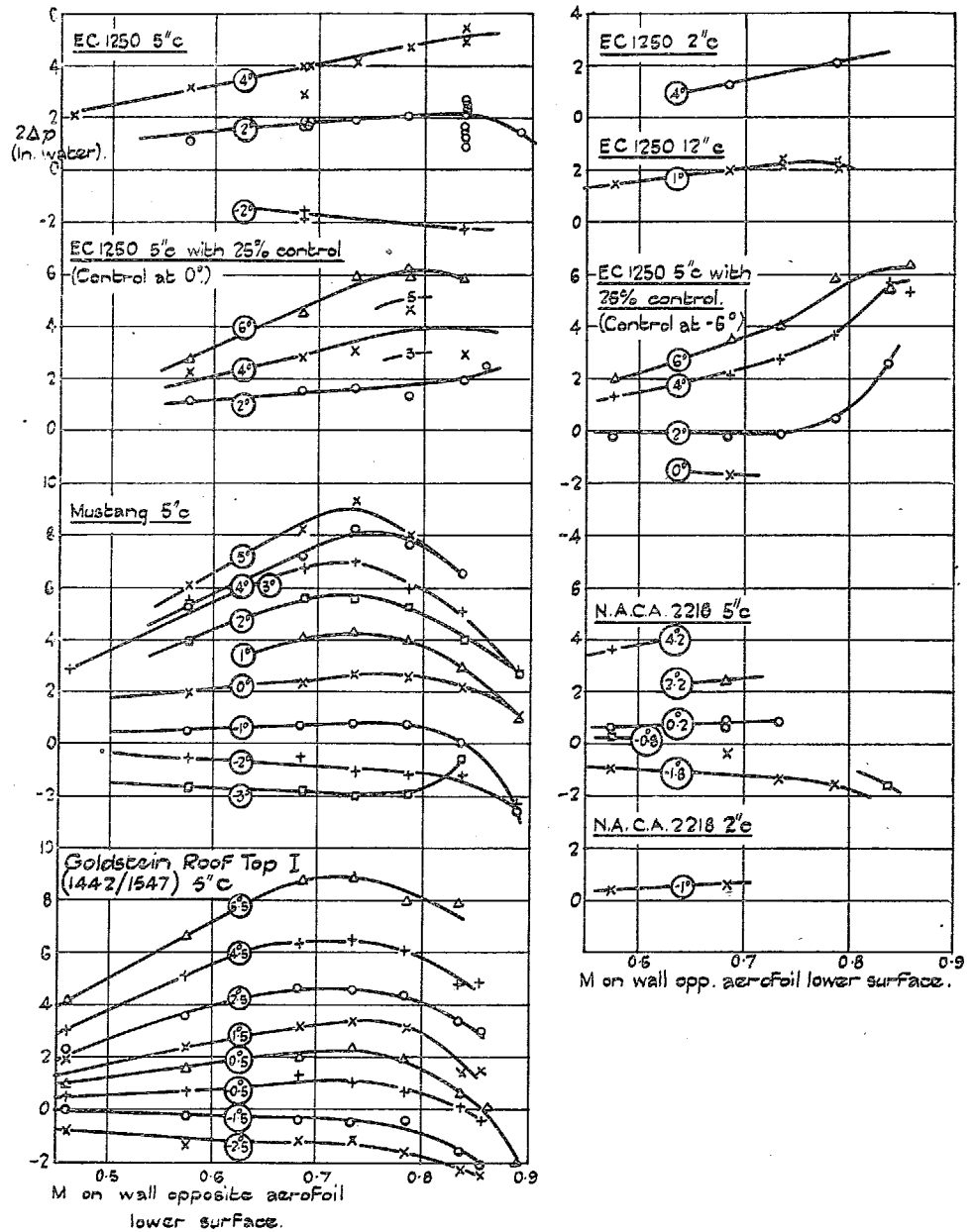

FIG. 12.—Constant Pressure Walls—Pressure Difference between the Two Walls. (— $2\Delta p$ is B side (opposite upper surface)—A side.)

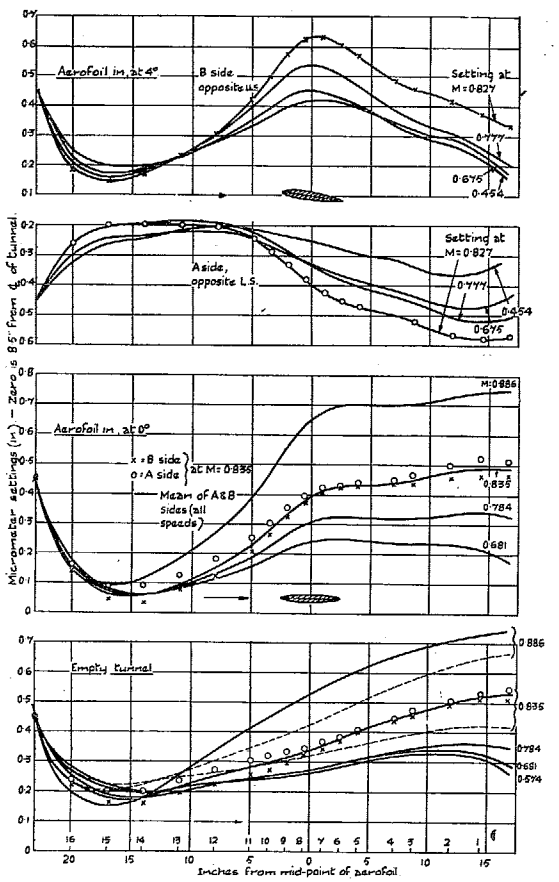

FIG. 13.—Wall Shapes for Constant Pressure. Aerofoil EC 1250 5-in. chord at 0 deg. and 4 deg.

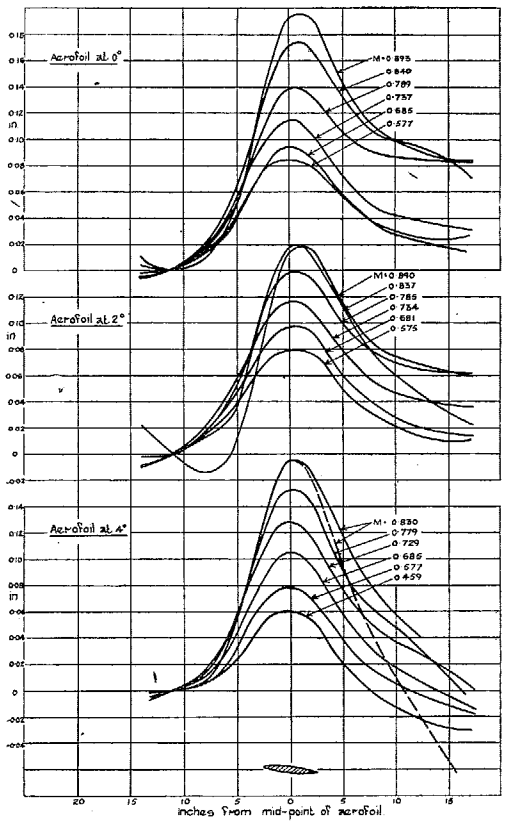

FIG. 14.—Wall Shapes for Constant Pressure—Blockage Effect with Aerofoil EC 1250 5-in. chord.

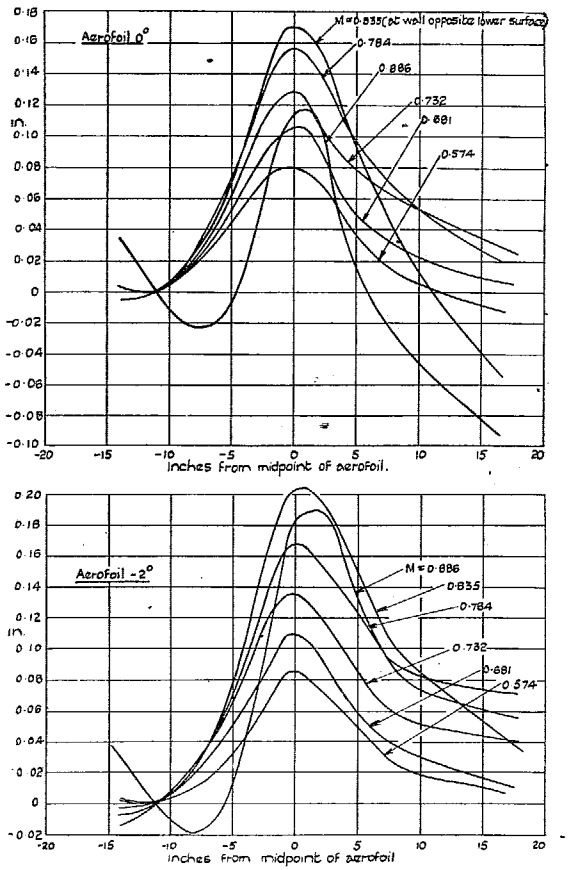

FIG. 15a.—Wall Shapes for Constant Pressure—Blockage Effect with Mustang Aerofoil.

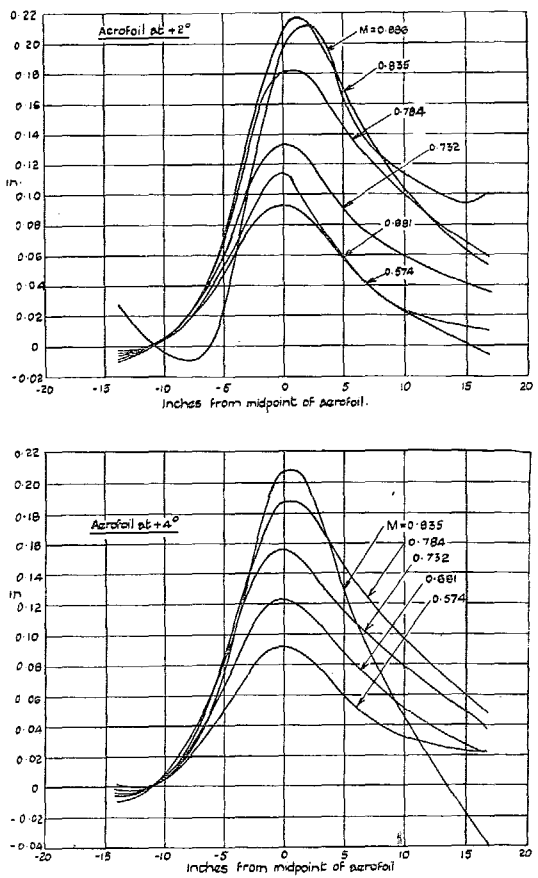

FIG. 15b.—Wall Shapes for Constant Pressure—Blockage Effect with Mustang Aerofoil.

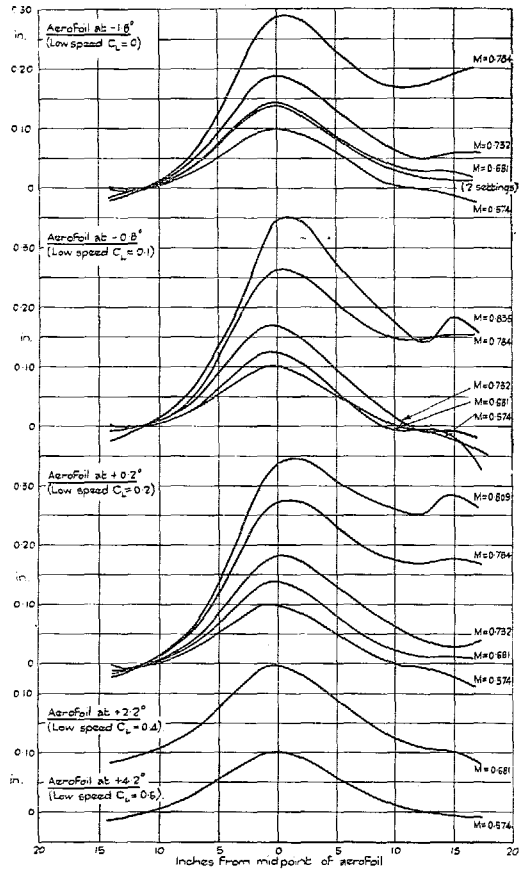

FIG. 16.—Wall Shapes for Constant Pressure—Blockage Effect with NACA 2218 5-in. chord Aerofoil.

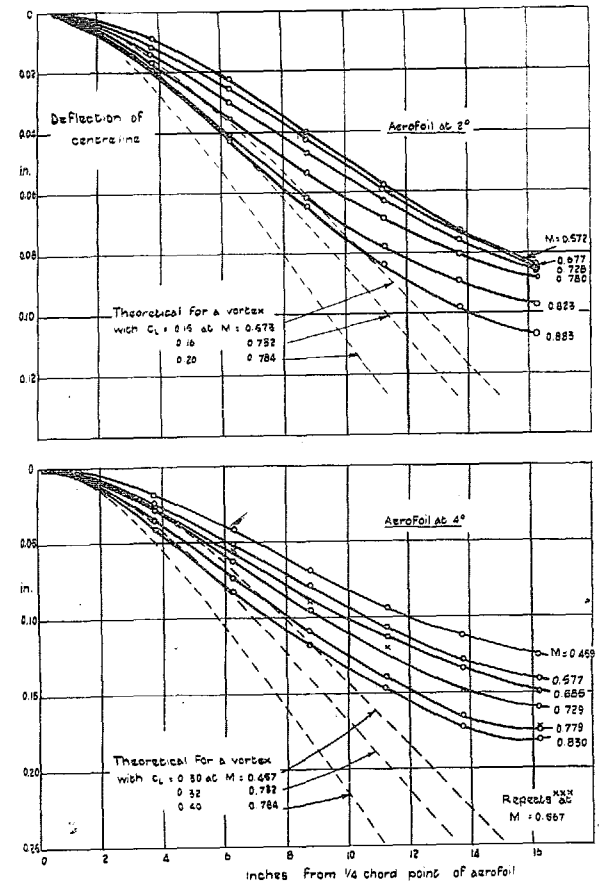

FIG. 17.—Wall Shapes for Constant Pressure—Lift Effect with Aerofoil EC 1250 5-in. chord.

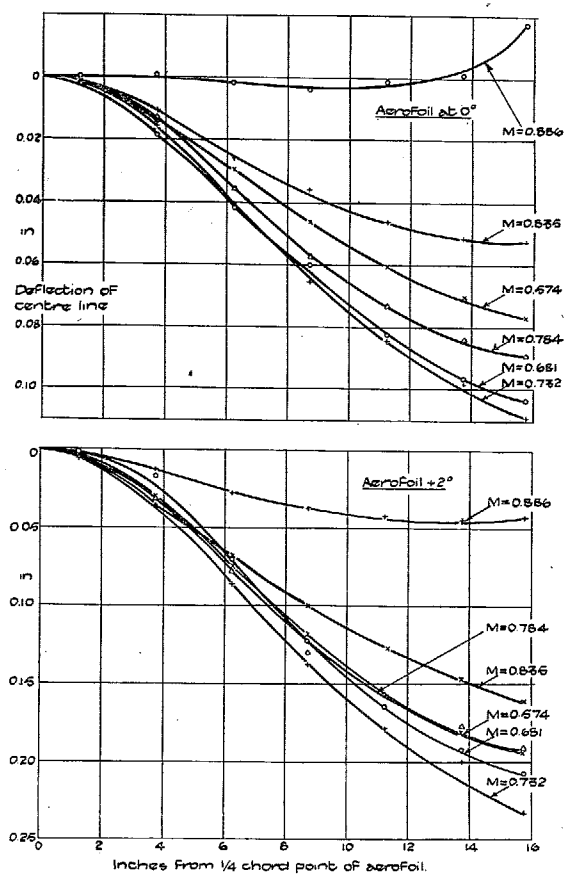

FIG. 18.—Wall Shapes for Constant Pressure—Lift Effect with Mustang Aerofoil 5-in. chord.

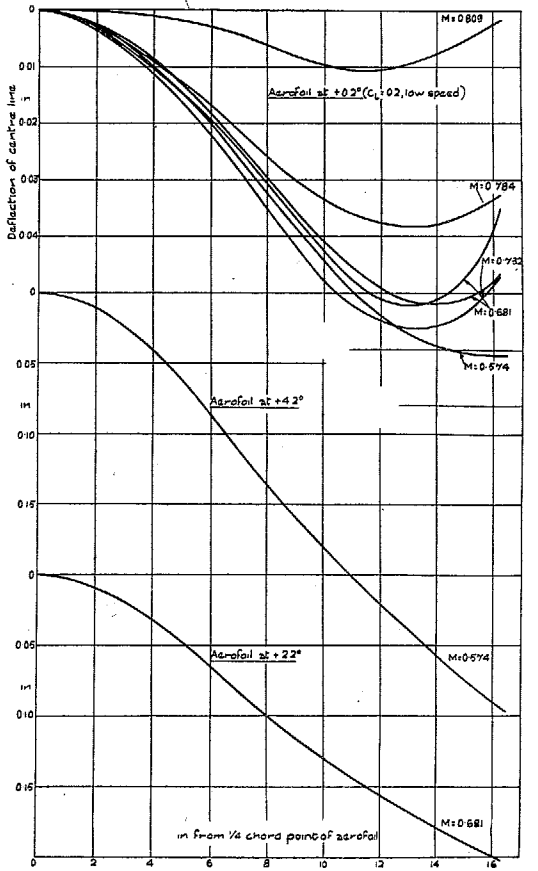

FIG. 19.—Wall Shapes for Constant Pressure—Lift Effect with NACA 2218 5-in. chord Aerofoil.

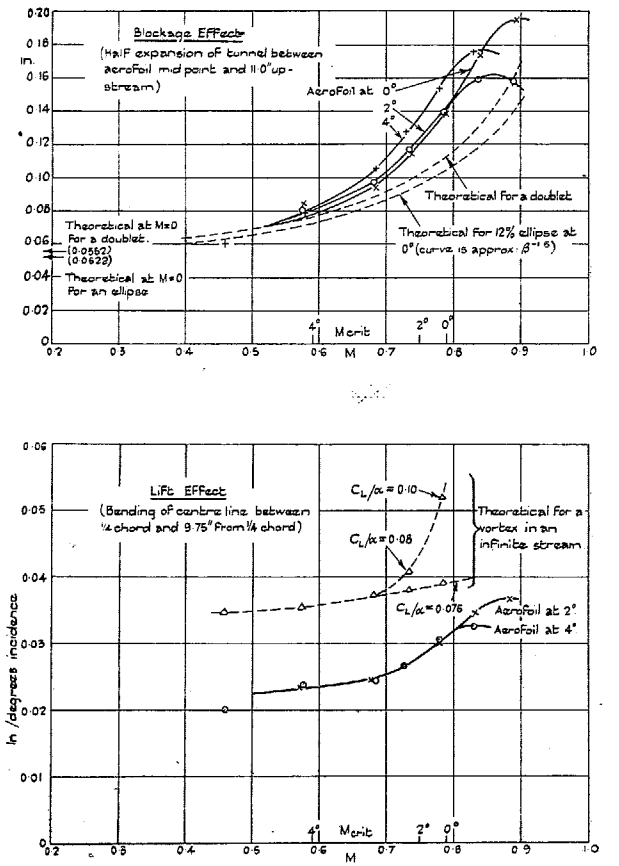

FIG. 20.—Wall Shapes for Constant Pressure—Displacement opposite Aerofoil EC 1250 5-in. chord.

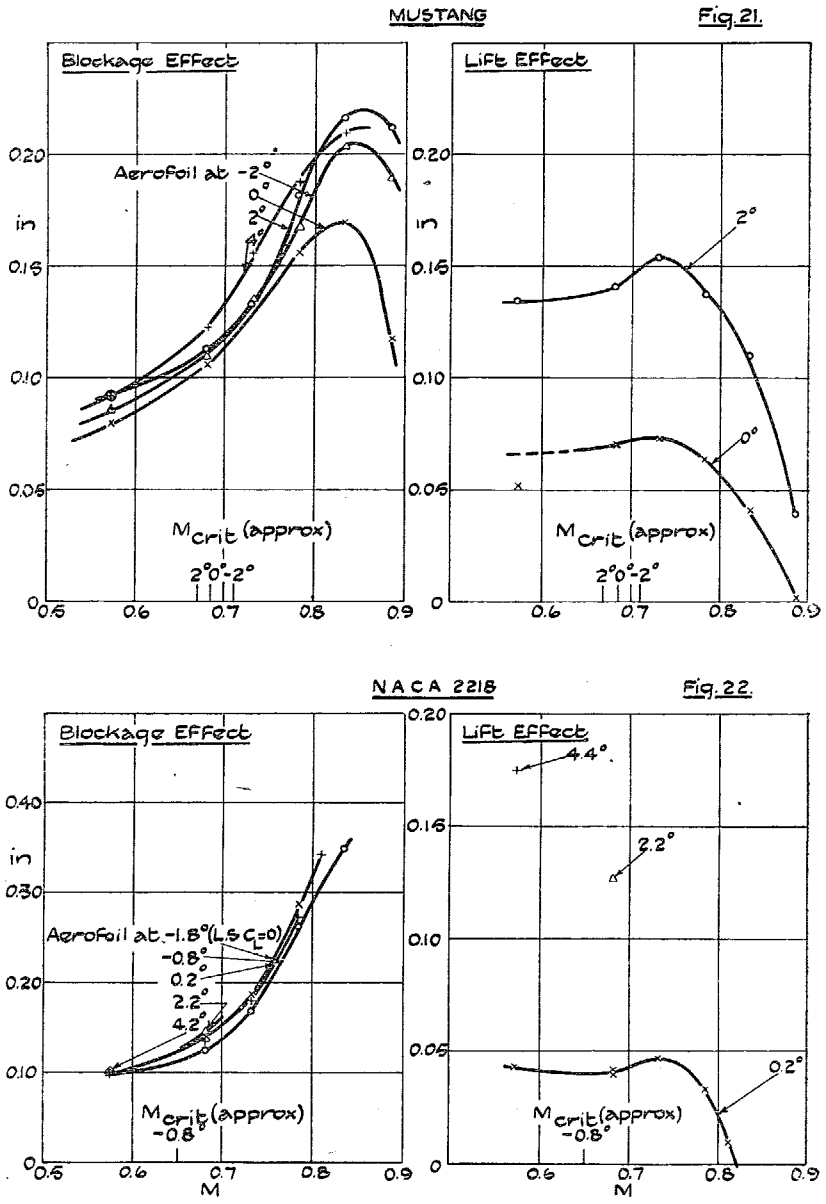

FIGS. 21 and 22.—Wall Shapes for Constant Pressure—Displacement opposite Mustang 5-in. chord and NACA 2218 5-in. chord Aerofoils.

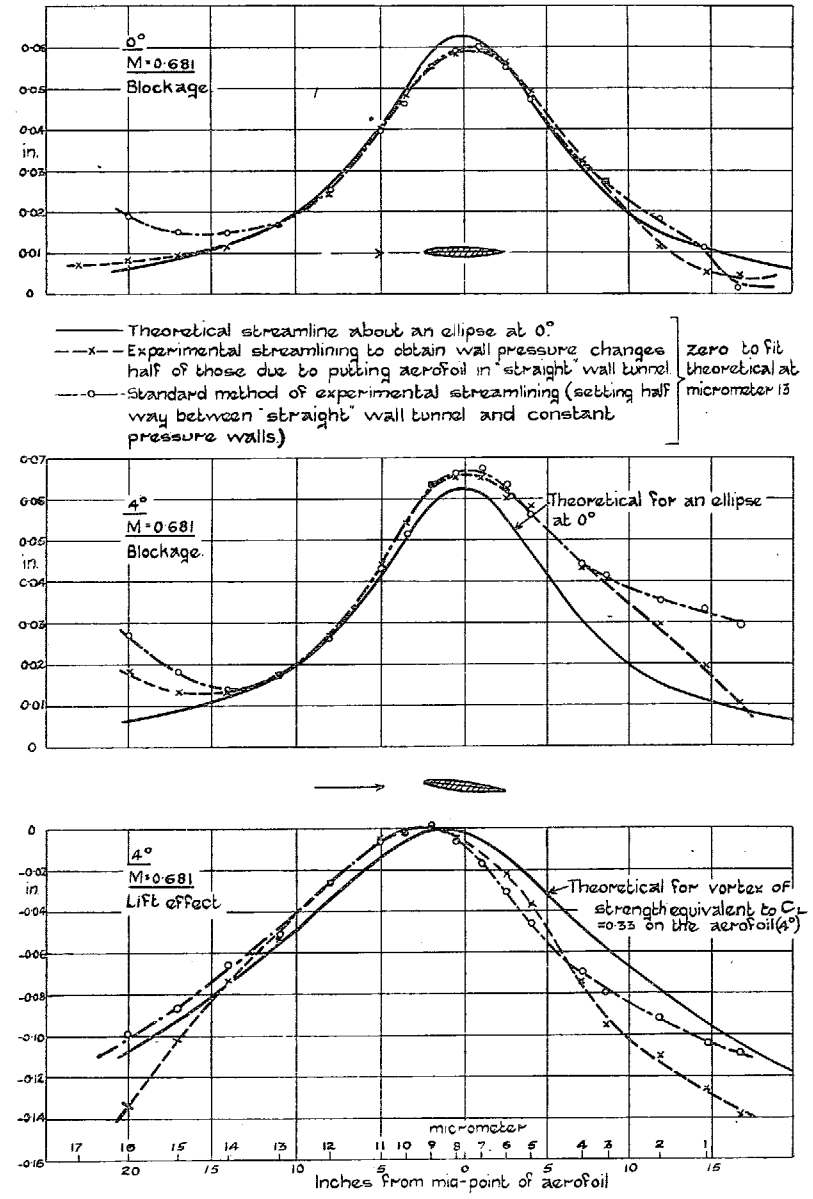

FIG. 23.—Comparison of Wall Shapes for Streamline Settings—Aerofoil EC 1250 5-in. chord at 0 deg. and 4 deg.

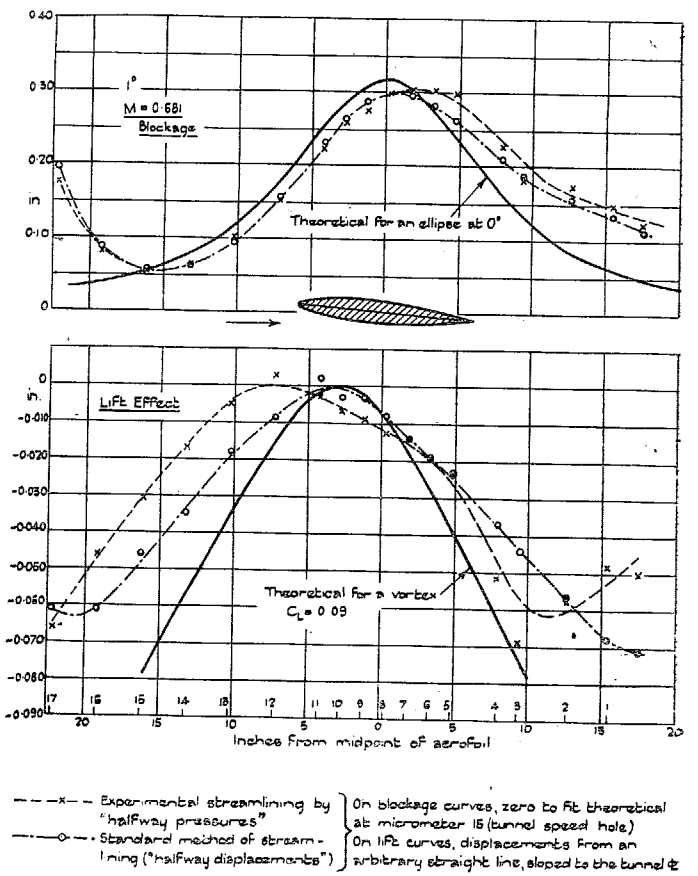

FIG. 24.—Comparison of Wall Shapes for Streamline Settings—EC 1250 12-in. chord at 1 deg.

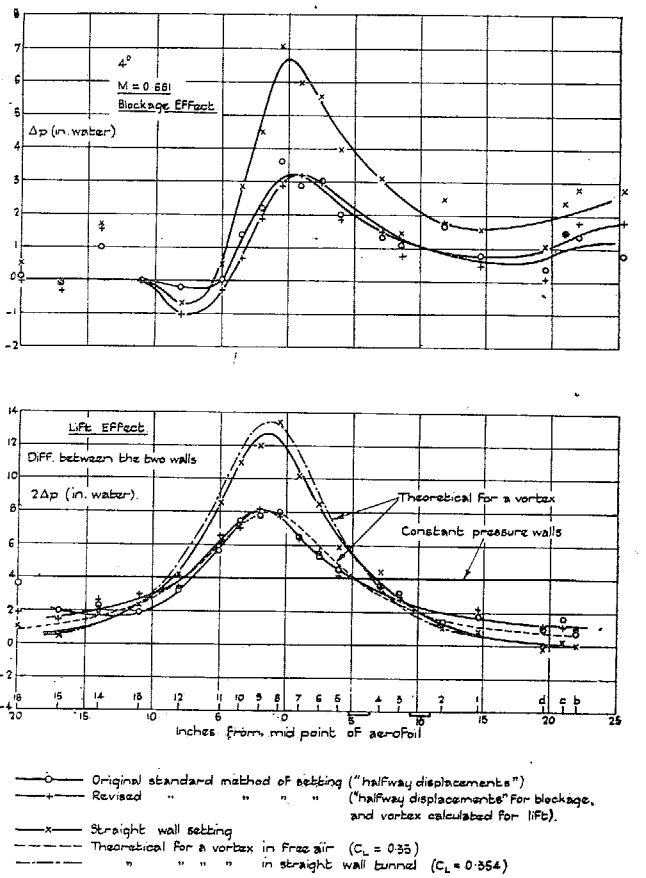

FIG. 25.—Pressures on Streamline Walls—EC 1250 5-in. chord at 4 deg.

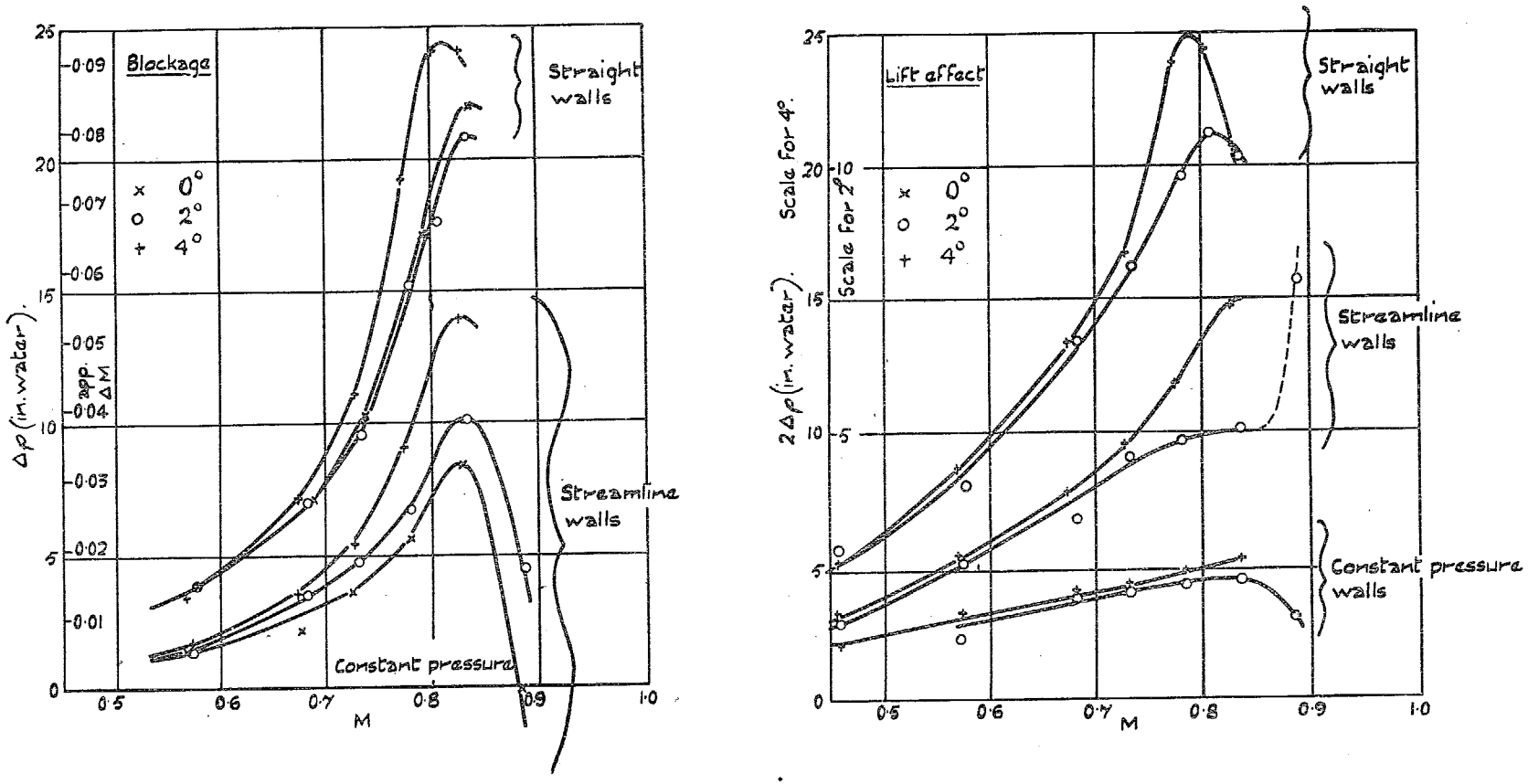

FIG. 26.—Pressures opposite EC 1250 5-in. chord with Streamline and Straight Walls.

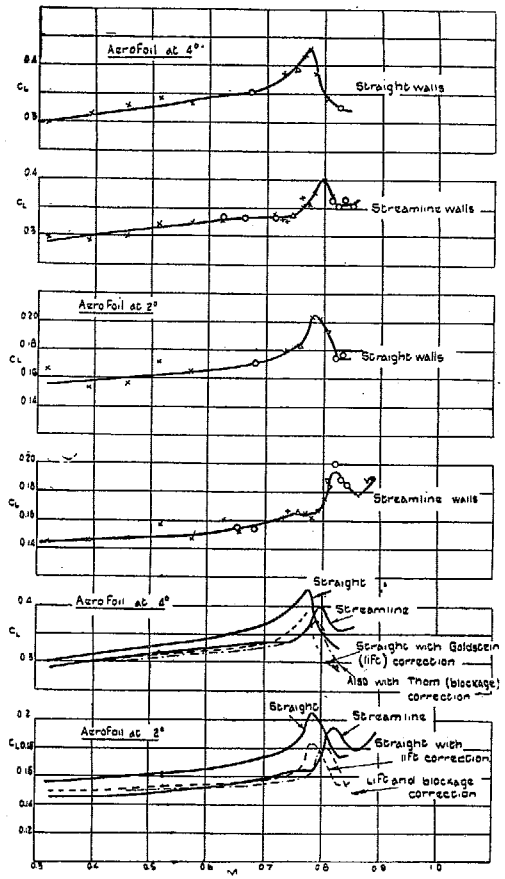

FIG. 27.—Comparison of Lift with Streamline and Straight Walls—EC 1250 5-in. chord.

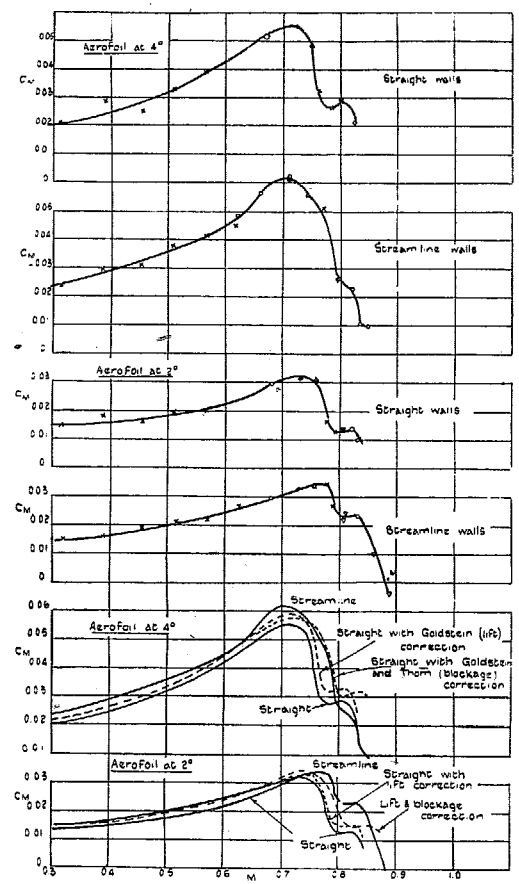

FIG. 28.—Comparison of Moment with Streamline and Straight Walls—EC 1250 5-in. chord.

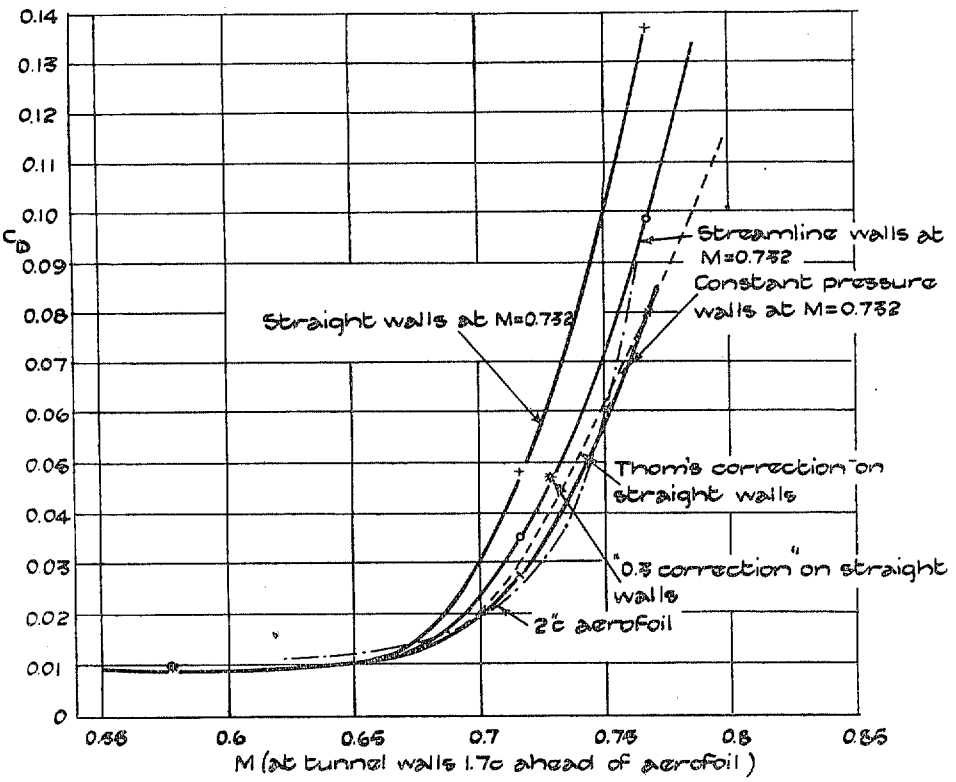

FIG. 29.—NACA 2218 5-in. chord Drag Variation with Wall Shape at C_L =0·1 (Low Speed) α = — 0·8 deg.

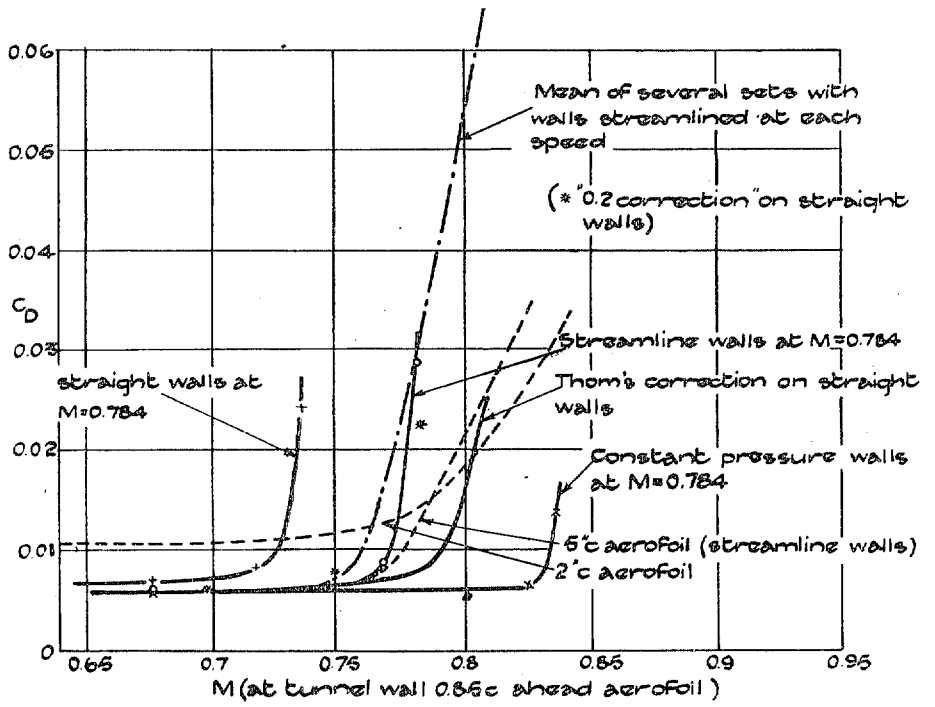

FIG. 30.—EC 1250 12-in. chord Drag Variation with Wall Shape at Zero Incidence.

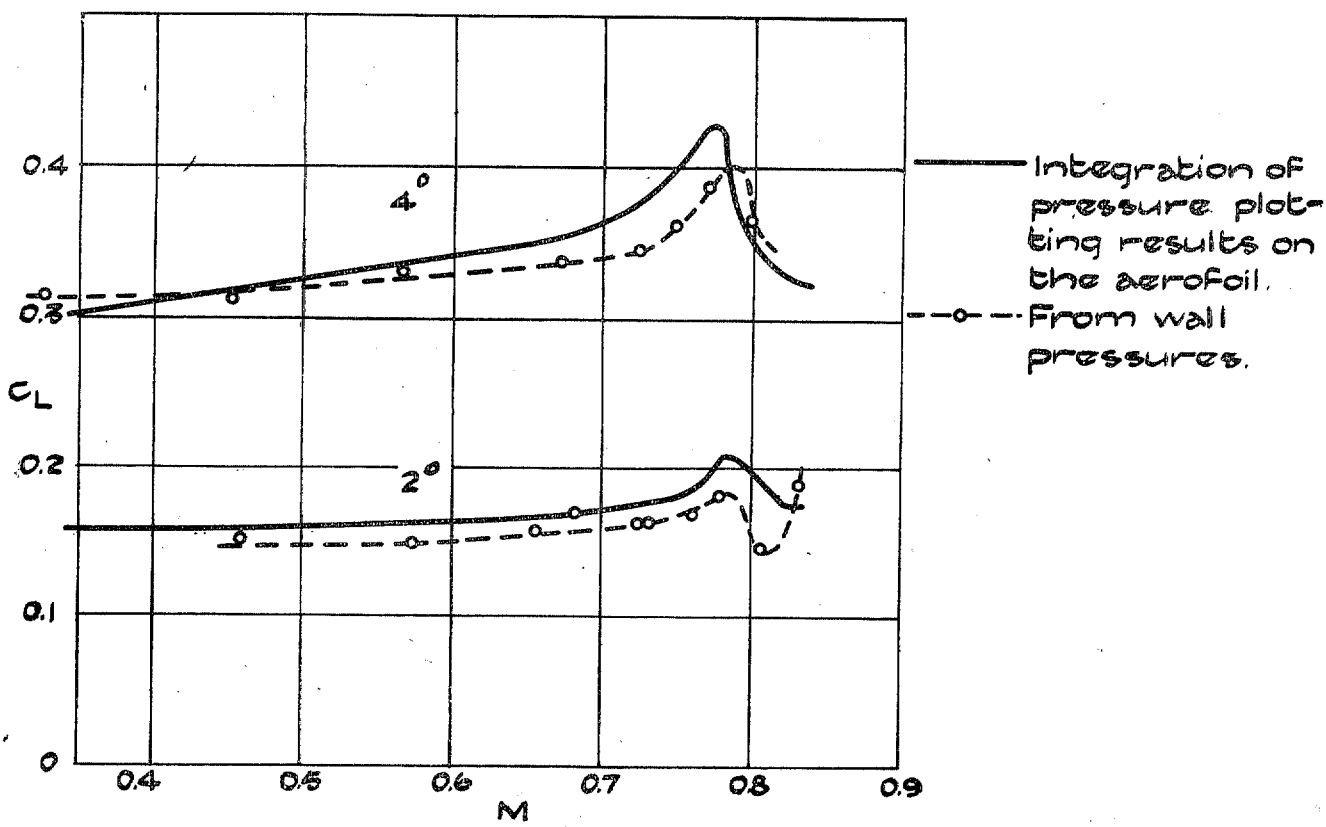

FIG. 31.—Lift from Wall Pressures (Straight Walls).

(74561) Wt. 9/7116 1/47 Hw. G.377/1